



1           **Recent changes in terrestrial water storage in the Upper Nile Basin: an**  
2           **evaluation of commonly used gridded GRACE products**

3  
4   **Mohammad Shamsudduha<sup>1,2</sup>, Richard G. Taylor<sup>2</sup>, Darren Jones<sup>3</sup>, Laurent Longuevergne<sup>4</sup>,**  
5           **Michael Owor<sup>5</sup> and Callist Tindimugaya<sup>6</sup>**

6  
7           <sup>1</sup>Institute for Risk and Disaster Reduction, University College London, UK

8           <sup>2</sup>Department of Geography, University College London, UK

9           <sup>3</sup>Centre for Geography, Environment and Society, University of Exeter, UK

10          <sup>4</sup>CNRS – UMR 6118 Géosciences Rennes, Université de Rennes 1, France

11          <sup>5</sup>Department of Geology & Petroleum Studies, Makerere University, Uganda

12          <sup>6</sup>Directorate of Water Resources Management, Ministry of Water & Environment, Uganda

13  
14                   Correspondence to: M. Shamsudduha (m.shamsudduha@ucl.ac.uk)

15  
16   **Abstract**

17   GRACE (Gravity Recovery and Climate Experiment) satellite data monitor large-scale changes  
18   in total terrestrial water storage ( $\Delta$ TWS) providing an invaluable tool where in situ observations  
19   are limited. Substantial uncertainty remains, however, in the amplitude of GRACE gravity  
20   signals and the disaggregation of  $\Delta$ TWS into individual terrestrial water stores (e.g. groundwater  
21   storage). Here, we test the phase and amplitude of GRACE  $\Delta$ TWS signals from 5 commonly-  
22   used gridded products (i.e., NASA's *GRCTellus*: CSR, JPL GFZ; JPL-Mascons; GRGS  
23   GRACE) using in situ data and modelled soil-moisture from the Global Land Data Assimilation  
24   System (GLDAS). The focus of this analysis is a large and accurately observed reduction in  
25    $\Delta$ TWS of 75 km<sup>3</sup> from 2004 to 2006 in Lake Victoria in the Upper Nile Basin. We reveal  
26   substantial variability in current GRACE products to quantify the reduction of  $\Delta$ TWS in Lake  
27   Victoria that ranges from 68 km<sup>3</sup> (GRGS) to 50 km<sup>3</sup> and 26 km<sup>3</sup> for JPL-Mascons and



28 *GRCTellus*, respectively. Representation of the phase in  $\Delta TWS$  in the Upper Nile Basin by  
29 GRACE products varies but is generally robust with GRGS, JPL-Mascons and *GRCTellus*  
30 (ensemble mean of CSR, JPL and GFZ time-series data) explaining 91 %, 85 %, and 77 % of the  
31 variance, respectively, in in-situ  $\Delta TWS$ . Resolution of changes in groundwater storage ( $\Delta GWS$ )  
32 from GRACE  $\Delta TWS$  is greatly constrained by both uncertainty in modelled changes in soil-  
33 moisture storage ( $\Delta SMS$ ) and the low annual amplitudes in  $\Delta GWS$  (e.g., 3.5 to 4.4 cm) observed  
34 in deeply weathered crystalline rocks underlying the Upper Nile Basin. Our study highlights the  
35 substantial uncertainty in the amplitude of  $\Delta TWS$  that can result from different data-processing  
36 strategies in commonly used, gridded GRACE products.

37

38 **Keywords:** GRACE products; terrestrial water storage; groundwater; hard-rock aquifers; Lake  
39 Victoria; Lake Kyoga; Sub-Saharan Africa

40

41

## 42 1. Introduction

43 Satellite measurements under the Gravity Recovery and Climate Experiment (GRACE) mission  
44 have, since March 2002 (Tapley et al., 2004), enabled remote monitoring of large-scale (~200  
45 000 km<sup>2</sup>) spatio-temporal changes in total terrestrial water storage ( $\Delta TWS$ ) at 10-day to monthly  
46 timescales (Longuevergne et al., 2013; Humphrey et al., 2016). Over the last 15 years, studies in  
47 basins around the world (Rodell and Famiglietti, 2001; Strassberg et al., 2007; Leblanc et al.,  
48 2009; Chen et al., 2010; Longuevergne et al., 2010; Frappart et al., 2011; Jacob et al., 2012;  
49 Shamsudduha et al., 2012; Arendt et al., 2013; Kusche et al., 2016) show that GRACE satellites  
50 trace natural (e.g., drought, floods, glaciers and ice melting, sea-level rise) and anthropogenic



51 (e.g., abstraction-driven groundwater depletion) influences on  $\Delta TWS$ . GRACE-derived TWS  
52 provides vertically-integrated water storage changes in all water-bearing layers (Wahr et al.,  
53 2004; Strassberg et al., 2007; Ramillien et al., 2008) that include (Eq. 1) surface water storage in  
54 rivers, lakes, and wetlands ( $\Delta SWS$ ), soil moisture storage ( $\Delta SMS$ ), ice and snow water storage  
55 ( $\Delta ISS$ ), and groundwater storage ( $\Delta GWS$ ). GRACE measurements have over the last decade  
56 become an important hydrological tool for quantifying basin-scale  $\Delta TWS$  (Güntner, 2008; Xie et  
57 al., 2012; Hu and Jiao, 2015) and are increasingly being used to assess spatio-temporal changes  
58 in specific water stores (Famiglietti et al., 2011; Shamsudduha et al., 2012; Jiang et al., 2014;  
59 Castellazzi et al., 2016; Long et al., 2016; Nanteza et al., 2016) where time-series records of  
60 other individual freshwater stores are available (Eq. 1).

61

$$62 \quad \Delta TWS_t = \Delta GWS_t + \Delta ISS_t + \Delta SWS_t + \Delta SMS_t \quad (1)$$

63

64 GRACE-derived  $\Delta TWS$  derive from monthly gravitational fields which can be represented as  
65 spherical harmonic coefficients that are noisy as depicted in north-south elongated linear features  
66 or “stripes” on monthly global gravity maps (Swenson and Wahr, 2006; Wang et al., 2016).  
67 Post-processing of GRACE SH data is therefore required. The most popular GRACE products  
68 are NASA’s *GRCTellus* land gravity solutions (i.e., spherical harmonics based CSR, JPL and  
69 GFZ), which require scaling factors to recover spatially smoothed TWS signals (Swenson and  
70 Wahr, 2006; Landerer and Swenson, 2012). Additionally, NASA’s new monthly gridded  
71 GRACE product, Mass Concentration blocks (i.e., Mascons), estimate terrestrial mass changes  
72 directly from inter-satellite acceleration measurements and can be used without further post-  
73 processing (Rowlands et al., 2010; Watkins et al., 2015). GRGS GRACE are also spherical



74 harmonic-based products available at a 10-day timestep and can also be used directly since  
75 gravity fields are stabilised during the processing of GRACE satellite data (Lemoine et al., 2007;  
76 Bruinsma et al., 2010).

77

78 Restoration of the amplitude of *GRCTellus* TWS data, dampened by spatial Gaussian filtering  
79 with a large smoothing radius (e.g., 300 to 500 km), is commonly achieved using scaling factors  
80 that derive from a priori model of freshwater stores, usually a global-scale Land-Surface Model  
81 or LSM (Long et al., 2015). However, signal-restoration methods are emerging that do not  
82 require hydrological model or LSM (Vishwakarma et al., 2016). Substantial uncertainty  
83 nevertheless persists in the magnitude of applied scaling factors (e.g., *GRCTellus*) and  
84 corrections (Long et al., 2015). In situ observations provide a valuable and necessary constraint  
85 to the scaling of TWS signals over a particular study area as no consistent basis for ground-  
86 truthing these factors exists.

87

88 The disaggregation of GRACE-derived  $\Delta$ TWS anomalies into individual water stores (Eq. 1) is  
89 commonly constrained by the limited availability of observations of terrestrial freshwater stores  
90 (i.e.,  $\Delta$ SWS,  $\Delta$ SMS,  $\Delta$ GWS,  $\Delta$ ISS). Indeed, a major source of uncertainty in the attribution of  
91 GRACE  $\Delta$ TWS derives from the continued reliance on modelled  $\Delta$ SMS derived from LSMs  
92 (i.e., CLM, NOAH, VIC, MOSAIC) under the Global Land Data Assimilation System or  
93 GLDAS (Rodell et al., 2004) and remote-sensing products (Shamsudduha et al., 2012; Khandu et  
94 al., 2016). Further, analyses of GRACE-derived  $\Delta$ GWS often assume  $\Delta$ SWS is limited (Kim et  
95 al., 2009) yet studies in the humid tropics and engineered systems challenge this assumption  
96 showing that it can overestimate  $\Delta$ GWS (Shamsudduha et al., 2012; Longuevergne et al., 2013).



97 Robust estimates of  $\Delta$ GWS from GRACE gravity signals have, to date, been developed in  
98 locations where  $\Delta$ SWS is well constrained by in situ observations and groundwater is used  
99 intensively for irrigation so that  $\Delta$ GWS comprises a significant ( $>10\%$ ) proportion of  $\Delta$ TWS  
100 (Leblanc et al., 2009; Famiglietti et al., 2011; Shamsudduha et al., 2012; Scanlon et al., 2015). In  
101 Sub-Saharan Africa (SSA), intensive groundwater withdrawals are restricted to a limited number  
102 of locations (e.g., irrigation schemes, cities) and constrained by low-storage, low-transmissivity  
103 aquifers in the deeply weathered crystalline rocks that underlie  $\sim 40\%$  of this region  
104 (MacDonald et al., 2012) including the Upper Nile Basin. Consequently, the ability of low-  
105 resolution GRACE gravity signals to trace  $\Delta$ GWS in these hard-rock environments is unclear. A  
106 recent study (Nanteza et al., 2016) applies NASA's *GRCTellus* (CSR GRACE) data over large  
107 basin areas ( $>300\,000\text{ km}^2$ ) of East Africa and argues that  $\Delta$ GWS can be estimated with  
108 sufficient reliability to characterise regional groundwater systems after accounting for  $\Delta$ SWS by  
109 satellite altimetry and  $\Delta$ SMS data from the GLDAS LSM ensemble (Rodell et al., 2004).

110

111 Here, we exploit a large-scale reduction and recovery in surface water storage that was recorded  
112 within Lake Victoria (Fig. 1), the world's second largest lake by surface area ( $67\,220\text{ km}^2$ )  
113 (UNEP, 2013) and eighth largest by volume ( $2\,760\text{ km}^3$ ) (Awange et al., 2008). This well-  
114 constrained reduction in  $\Delta$ SWS comprises a decline in lake level of 1.2 m between May 2004  
115 and February 2006, equivalent to a lake-water volume ( $\Delta$ SWS) loss of  $81\text{ km}^3$  that resulted, in  
116 part, from excessive dam releases (Fig. 2). We test the ability of current GRACE products to  
117 represent the amplitude and phase of this voluminous and well-constrained change in freshwater  
118 storage. Our analysis focuses on both the Lake Victoria Basin (hereafter LVB) ( $256\,100\text{ km}^2$ )  
119 and Lake Kyoga Basin (hereafter LKB) ( $79\,270\text{ km}^2$ ) (Fig. 1). Applying in situ observations of



120  $\Delta$ SWS and  $\Delta$ GWS combined with simulated  $\Delta$ SMS by the GLDAS LSMs, we assess: (1) the  
121 ability of current gridded GRACE products (i.e., *GRCTellus*, JPL-Mascons, GRGS GRACE) to  
122 measure a well constrained  $\Delta$ TWS in the Upper Nile Basin from 2003 to 2012 focusing on the  
123 unintended experiment within the LVB from 2004 to 2006; and (2) the sensitivity of a  
124 disaggregated GRACE  $\Delta$ TWS signals to trace  $\Delta$ GWS in a deeply weathered crystalline rock  
125 aquifer systems underlying the Upper Nile Basin.

126

127

## 128 **2. The Upper Nile Basin**

### 129 **2.1 Hydroclimatology**

130 The Upper Nile Basin, the headwater area of the ~3 400 000 km<sup>2</sup> Nile Basin (Awange et al.,  
131 2014), includes both the Lake Victoria Basin (LVB) and Lake Kyoga Basin (LKB). Mean annual  
132 rainfall over the entire basin varies from 650 to 2900 mm (TRMM monthly rainfall; 2003–2012)  
133 with an average of 1300 mm ( $\sigma=354$  mm) (Fig. 3). Mean annual gauged rainfall at different  
134 stations, Jinja, Bugondo and Entebbe measured is 1195, 1004 and 1541 mm, respectively (Owor  
135 et al., 2011). Rainfall over Lake Victoria is typically 25–30 % greater than that measured in the  
136 surrounding catchment (Fig. 3), which is partially explained by the nocturnal ‘lake breeze’ effect  
137 (Yin and Nicholson, 1998; Nicholson et al., 2000; Owor et al., 2011).

138

139 Estimates of mean annual evaporation from the surface of Lake Victoria vary from 1260 mm  
140 (UNEP, 2013) to 1566 mm (Hoogeveen et al., 2015) whereas mean annual evaporation from the  
141 surface of Lake Kyoga is estimated to vary from 1205 mm (Brown and Sutcliffe, 2013) to 1660  
142 mm (Hoogeveen et al., 2015). Evapotranspirative fluxes from the surrounding swamps in Lake



143 Kyoga are estimated to be much higher and approximately 2230 mm yr<sup>-1</sup> (Brown and Sutcliffe,  
144 2013).

145

146 Annual rainfall is predominantly bimodal in distribution (Fig. 4) with two distinct rainy seasons  
147 driven by the movement of the Intertropical Convergence Zone (ITCZ) (Awange et al., 2013).

148 Long rains (March to May) and short rains (September to November) account for approximately  
149 40% and 25% of annual rainfall respectively (Basalirwa, 1995; Indeje et al., 2000). The latter  
150 rainfalls are particularly influenced by El-Niño Southern Oscillation (ENSO) and Indian Ocean  
151 Dipole (IOD). GRACE-derived  $\Delta$ TWS within the LVB shows a statistical association ( $R^2$ ) of  
152 0.56 with ENSO and 0.48 with IOD (Awange et al., 2014).

153

## 154 **2.2 Lakes Victoria and Kyoga**

155 Located between 31°39' E and 34°53' E longitudes, and 0°20' N and 3°00' S latitudes, Lake  
156 Victoria (Fig. 1) is located in Tanzania, Uganda and Kenya where each accounts for 51 %, 43 %  
157 and 6 % of lake surface area respectively (Kizza et al., 2012). Lake Victoria is relatively shallow  
158 with a mean depth of ~40 m and a maximum depth of 84 m (UNEP, 2013) akin to many shallow,  
159 open surface-water bodies as well as permanent and seasonal wetlands occupying low relief  
160 plateau across the Great Lakes Region of Africa (Owor et al., 2011). Moreover, the western and  
161 northwestern lake bathymetry is characterised by even shallower depths of between 4 and 7 m  
162 (Owor, 2010). Hydrologically, lake input is dominated by direct rainfall (84 % of total input); the  
163 remainder derives primarily from river inflows as direct groundwater inflow (<1 %) is negligible  
164 (Owor et al., 2011). Approximately 25 major rivers flow into Lake Victoria with a total  
165 catchment area of ~194 000 km<sup>2</sup>; the largest tributary, River Kagera, contributes ~30 % of total



166 river inflows (Sene and Plinston, 1994). Lake Victoria outflow to Lake Kyoga occurs at Jinja  
167 (Fig. 1).  
168  
169 Lake Kyoga (Fig. 1), located between 32°10' E and 34°20' E longitudes, and 1°00' N and 2°00'  
170 N latitudes, has a mean area of 1 720 km<sup>2</sup> with an estimated mean volume of 12 km<sup>3</sup> (Owor,  
171 2010; UNEP, 2013). According to the recent global *HydroSHEDS* (Hydrological data and maps  
172 based on shuttle elevation derivatives at multiple Scales) database, the Lake Kyoga has a total  
173 surface area of 2 729 km<sup>2</sup> (Lehner et al., 2008). Lake Kyoga comprises lake-zone and flow-  
174 through conduit areas. The lake zone in Lake Kyoga is very shallow with a mean depth of 3.5 to  
175 4.5 m (Owor, 2010). Lake Kyoga has a through-flow channel (mean depth 7 to 9 m) where the  
176 main Victoria Nile River flows (Owor, 2010) and acts as a linear reservoir with the annual water  
177 balance predominantly governed by the discharge of the Victoria Nile from Lake Victoria. Lake  
178 Kyoga has a through-flow channel (mean depth 7–9 m) where the main Victoria Nile River  
179 flows (Owor, 2010). Whilst numerous rivers flow into Lake Kyoga (e.g. Rivers Mpologoma,  
180 Awoja, Omunyal, Abalang, Olweny, Sezibwa and Enget) (Owor, 2010), the majority contributes  
181 a fraction of their former volume upon reaching the lake (Krishnamurthy and Ibrahim, 2013)  
182 due, in part, to evapotranspirative losses from fringe swamp areas (4 510 km<sup>2</sup>) surrounding the  
183 lake (UNEP, 2013).

184

### 185 **2.3 Hydrogeological setting**

186 The Upper Nile Basin is underlain primarily by deeply weathered crystalline rock aquifer  
187 systems that have evolved through long-term, tectonically-driven cycles of deep weathering and  
188 erosion (Taylor and Howard, 2000). Groundwater occurs within unconsolidated regoliths or





189 'saprolite' and, below this, in fractured bedrock, known as 'saprock'. Bulk transmissivities of the  
190 saprolite and saprock aquifers are generally low ( $1$  to  $20 \text{ m}^2 \text{ d}^{-1}$ ) (Taylor and Howard, 2000;  
191 Owor, 2010) and field estimates of the specific yield of the saprolite, the primary source of  
192 groundwater storage in these aquifer systems, are  $2 \%$  based on pumping-tests with tracers  
193 (Taylor et al., 2010) and magnetic resonance sounding experiments (Vouillamoz et al., 2014).  
194 Borehole yields are highly variable but generally low ( $0.5$  to  $20 \text{ m}^3 \text{ h}^{-1}$ ) yet are of critical  
195 importance to the provision of safe drinking water.

196

#### 197 **2.4 An observed reduction in TWS in the LVB**

198 In 1954, the construction of the Nalubaale Dam (formerly Owen Falls Dam) at the outlet of Lake  
199 Victoria at Jinja transformed the lake into a controlled reservoir (Sene and Plinston, 1994).  
200 Operated as a run-of-river hydroelectric project to mimic pre-dam outflows, the 'Agreed Curve'  
201 between Uganda and Egypt dictated dam releases that were controlled on a 10-day basis and  
202 generally adhered to, with compensatory discharge releases to minimise any departures, until the  
203 construction of the Kiira dam at Jinja in 2002 (Sene and Plinston, 1994; Owor et al., 2011).

204

205 The combined discharge of the Nalubaale and Kiira Dams enabled total dam releases (Fig. 2) to  
206 substantially exceed the Agreed Curve (Sutcliffe and Petersen, 2007) and between May 2004 and  
207 February 2006 the lake level dropped by  $1.2 \text{ m}$  (equivalent  $\Delta\text{SWS}$  loss of  $81 \text{ km}^3$ ) (Owor et al.,  
208 2011). Mean annual releases were  $1387 \text{ m}^3 \text{ s}^{-1}$  ( $+162 \%$  of Agreed Curve) in 2004 and  $1114 \text{ m}^3 \text{ s}^{-1}$   
209  $(+148 \%$  of Agreed Curve) in 2005. Sharp reductions in dam releases in 2006 helped to arrest  
210 and reverse the lake-level decline with lake levels stabilising by early 2007.

211



## 212 3. Data and Methods

### 213 3.1 Datasets

214 We use publicly available time-series records of: (1) GRACE TWS solutions from a number of  
215 data processing and dissemination centres including NASA's *GRCTellus* land solutions (RL05  
216 for CSR, GFZ (version DSTvSCS1409), RL05.1 for JPL (version DSTvSCS1411), JPL-Mascons  
217 solution (version RL05M\_1.MSCNv01)), and the French National Centre for Space Studies  
218 (CNES) GRGS (version GRGS RL03-v1); (2) NASA's Global Land Data Assimilation System  
219 (GLDAS) simulated soil moisture data from 3 global land surface models (LSMs) (CLM,  
220 NOAH, VIC); and (3) precipitation data from NASA's Tropical Rainfall Measuring Mission  
221 (TRMM) satellite mission. We also employ in-situ observations of lake levels and groundwater  
222 levels from a network of gauges and monitoring wells operated by the Ministry of Water and  
223 Environment in Entebbe (Uganda). Datasets are described briefly below.

224

#### 225 3.1.1 Delineation of basin study areas

226 Delineation of the Lake Victoria Basin (LVB) and Lake Kyoga Basin (LKB) was conducted in  
227 Geographic Information System (GIS) under ArcGIS (v.10.3.1) environment using the  
228 'Hydrological Basins in Africa' datasets derived from *HydroSHEDS* database (available at  
229 <http://www.hydrosheds.org/>) (Lehner et al., 2006, 2008). Regional water bodies including Lakes  
230 Victoria and Kyoga (Fig. 1) were spatially defined by the Inland Water dataset available globally  
231 at country scale from DIVA-GIS (Hijmans et al., 2012). Computed areas of the basins and lake  
232 surface areas are summarised in Table 1 along with previously estimated figures from other  
233 studies.

234



235 **3.1.2 GRACE-derived terrestrial water storage (TWS)**

236 Twin GRACE satellites provide monthly gravity variations interpretable as  $\Delta TWS$  (Tapley et  
237 al., 2004) with an accuracy of  $\sim 1.5$  cm (Equivalent Water Thickness or Depth) when spatially  
238 averaged (Wahr et al., 2006). In this study, we apply 5 different monthly GRACE solutions for  
239 the period of January 2003 to December 2012: post-processed, gridded ( $1^\circ \times 1^\circ$ ) GRACE-TWS  
240 time-series records from 3 *GRCTellus* land solutions from CRS, JPL and GFZ processing centres  
241 (available at <http://grace.jpl.nasa.gov/data>) (Swenson and Wahr, 2006; Landerer and Swenson,  
242 2012), JPL-Mascons (Watkins et al., 2015; Wiese et al., 2015), and GRGS GRACE products  
243 (CNES/GRGS release RL03-v1) (Biancale et al., 2006).

244

245 *GRCTellus* land datasets are post-processed from two versions, RL05 and RL05.1 of spherical  
246 harmonics released by the University of Texas at Austin Centre for Space Research (CSR) and  
247 the German Research Centre for Geosciences Potsdam (GFZ), and the NASA's Jet Propulsion  
248 Laboratory (JPL) respectively. *GRCTellus* datasets are available at monthly timestep at a spatial  
249 resolution of  $1^\circ \times 1^\circ$  grids ( $\sim 111$  km at equator).

250

251 Post-processing of *GRCTellus* GRACE datasets primarily involve (i) removal of atmospheric  
252 pressure or mass changes based on the European Centre for Medium-Range Weather Forecasts  
253 (ECMWF) model; (ii) a glacial isostatic adjustment (GIA) correction based on a viscoelastic 3-D  
254 model of the Earth (Geruo et al., 2013); and (iii) an application a destriping filter plus a 300-km  
255 Gaussian to minimise the effect of correlated errors (i.e., destriping) manifested by N-S  
256 elongated stripes in GRACE monthly maps. However, the use of a large spatial filter and  
257 truncation of spherical harmonics leads to energy removal so scaling coefficients or factors are



258 applied to the GRACE-derived TWS data in order to restore attenuated signals (Landerer and  
259 Swenson, 2012). Dimensionless scaling factors are also provided as  $1^\circ \times 1^\circ$  bins that derive from  
260 the Community Land Model (CLM4.0) (Landerer and Swenson, 2012).  
261  
262 *GRCTellus* JPL-Mascons (version RL05M\_1.MSCNv01) data processing also involves a glacial  
263 isostatic adjustment (GIA) correction based on a viscoelastic 3-D model of the Earth (Geruo et  
264 al., 2013). JPL-Mascons applies no spatial filtering as JPL-RL05M directly relates inters-satellite  
265 range-rate data to mass concentration blocks or Mascons to estimate global monthly gravity  
266 fields in terms of equal area  $3^\circ \times 3^\circ$  mass concentration functions to minimise measurement  
267 errors. The use of Mascons and the special processing result in better signal-to-noise ratios of the  
268 mascon fields compared to the conventional spherical harmonic solutions (Watkins et al., 2015).  
269 For convenience, gridded Mascons fields are provided at a spatial sampling of  $0.5^\circ$  in both  
270 latitude and longitude ( $\sim 56$  km at the equator). As with *GRCTellus* GRACE datasets the  
271 neighbouring grid cells are not ‘independent’ of each other and cannot be interpreted  
272 individually at the  $1^\circ$  or  $0.5^\circ$  grid scale (Watkins et al., 2015).  
273  
274 GRGS/CNES GRACE monthly products (version RL03-v1) are processed and made publicly  
275 available (<http://grgs.obs-mip.fr/grace>) by the French Government space agency, National Centre  
276 for Space Studies or Centre National d' Études Spatiales (CNES). The post-processing of GRGS  
277 data involves taking into account of gravitational variations such as Earth tides, ocean tides, and  
278 3D gravitational potential of the atmosphere and ocean masses (Bruinsma et al., 2010). The  
279 remaining signals for time-varying gravity fields therefore represent changes in terrestrial  
280 hydrology including snow cover, baroclinic oceanic signals and effects of post-glacial rebound



281 (Biancale et al., 2006; Lemoine et al., 2007). Further details on the Earth's mean gravity-field  
282 models can be found on the official website of GRGS/LAGEOS (<http://grgs.obs-mip.fr/grace/>).  
283  
284 GRACE satellites were launched in 2002 to map the variations in Earth's gravity field over its 5-  
285 year lifetime but both satellites are still in operation even after more than 14 years. However,  
286 active battery management since 2011 has led the GRACE satellites to be switched off every 5–6  
287 months for 4–5 week durations in order to extend its total lifespan (CSR, 2016). As a result,  
288 GRACE  $\Delta$ TWS time-series data have some missing records that are linearly interpolated  
289 (Shamsudduha *et al.*, 2012). In this study, we derive  $\Delta$ TWS time-series data as equivalent water  
290 depth (cm of H<sub>2</sub>O) using the basin boundaries (GIS shapefiles) for masking the 1° × 1° grids.

291

### 292 **3.1.3 Soil moisture storage (SMS)**

293 NASA's Global Land Data Assimilation System (GLDAS) is an uncoupled land surface  
294 modelling system that drives multiple land surface models (GLDAS LSMs: CLM, NOAH, VIC  
295 and MOSAIC) globally at high spatial and temporal resolutions (3-hourly to monthly at 0.25° ×  
296 0.25° grid resolution) and produces model results in near-real time (Rodell et al., 2004). These  
297 LSMs provide a number of output variables which include soil moisture storage (SMS). Similar  
298 to the approach applied in the analysis of GRACE-derived  $\Delta$ TWS analysis in the Bengal Basin  
299 (Shamsudduha et al., 2012), we apply simulated monthly  $\Delta$ SMS records at a spatial resolution of  
300 1° × 1° from 3 GLDAS LSMs: the Community Land Model (CLM, version 2) (Dai et al., 2003),  
301 NOAH (version 2.7.1) (Ek et al., 2003) and the Variable Infiltration Capacity (VIC) model  
302 (version 2.7.1) (Liang et al., 2003). The respective depths of modelled soil profiles are 3.4 m, 2.0  
303 m, and 1.9 m in CLM (10 vertical layers), NOAH (4 vertical layers), and VIC (version 1.0) (3



304 vertical layers). Because of the absence of in situ soil moisture data in the study areas we apply  
305 an ensemble mean of the aforementioned 3 LSMs-derived simulated  $\Delta$ SMS time-series records  
306 in order to disaggregate GRACE  $\Delta$ TWS signals.

307

#### 308 **3.1.4 Surface water storage (SWS)**

309 Daily time-series of  $\Delta$ SWS are computed from in situ (gauged) lake-level observations at Jinja  
310 for Lake Victoria and Bugondo for Lake Kyoga (Fig.s 1 and 2) compiled by the Ugandan  
311 Ministry of Water and Environment (Directorate of Water Resources Management). Mean  
312 monthly anomalies for the period of 2003–2012 were computed as an equivalent water depth  
313 using Eq. (2). Missing data in the time series (2003–2012) records are linearly interpolated. For  
314 instance, in case of monthly  $\Delta$ SWS derived from Lake Kyoga water levels, there is one missing  
315 record (December 2005).

316

$$317 \quad \Delta SWS = \Delta Lake Level \times \left( \frac{Lake Area}{Total Basin Area} \right) \quad (2)$$

318

#### 319 **3.1.5 Groundwater storage (GWS)**

320 Time series of  $\Delta$ GWS are constructed from in situ piezometric records from 6 monitoring wells  
321 located in LVB and LKB where near-continuous, daily observations exist from 2003 to 2012 and  
322 have been compiled by the Ugandan Ministry of Water and Environment (Directorate of Water  
323 Resources Management) (Owor et al., 2009; Owor et al., 2011). Monitoring boreholes were  
324 installed into weathered, crystalline rock aquifers that underlie much of LVB and LKB, and are  
325 remote from local abstraction. As such, they represent variations in groundwater storage



326 influenced primarily by climate variability. Mean monthly anomalies of  $\Delta GWS$ , normalised to  
327 2003–2012, were derived from near-continuous, daily observations at Entebbe, Rakai and  
328 Nkokonjeru for LVB and at Apac, Pallisa and Soroti for LKB (Fig. 1; Table 2). These time series  
329 data are a sub-set of the total number of available monitoring-well records in the LVB and LKB  
330 following a rigorous review of groundwater-level records conducted at a dedicated workshop at  
331 the Ministry of Water & Environment in January 2013. These records represent shallow  
332 groundwater-level observations within the saprolite that is dynamically connected to surface  
333 waters (Owor et al. 2011). The limited spatial coverage in quality-controlled piezometry,  
334 especially for the LVB, represents an important limitation in our analysis. Mean monthly  
335 anomalies were translated into an equivalent water depth (Eq. 3) by applying a range of specific  
336 yield ( $S_y$ ) values (1–6 % with an average of 3 %) although estimates of  $S_y$  in hard-rock  
337 environments are observed to vary from < 2% to 8 % (Taylor et al., 2010; Taylor et al., 2013;  
338 Vouillamoz et al., 2014) using Eq. (3). Missing data in the time series were linearly interpolated.  
339 In case of monthly  $\Delta GWS$  that derived from borehole ( $n=6$ ) observations, missing records range  
340 from 1–9 months (120 months in 2003–2012) with three boreholes (Soroti, Rakai and  
341 Nkonkonjero) with time-series records ending in June–July 2010.

342

$$343 \quad \Delta GWS = \Delta h * S_y * \left( \frac{Land\ Area}{Total\ Basin\ Area} \right) \quad (3)$$

344

### 345 **3.1.6 Rainfall data**

346 We apply Tropical Rainfall Measuring Mission (TRMM) (Huffman et al., 2007) monthly  
347 product (3B43 version 7) for the period of 2003 to 2012 at  $0.25^\circ \times 0.25^\circ$  spatial resolution and  
348 aggregate to  $1^\circ \times 1^\circ$  grids over LVB and LKB. General climatology of the Upper Nile Basin is



349 represented by long-term (2003–2012) mean annual rainfall (Fig. 3) and seasonal rainfall pattern  
350 (Fig. 4). TRMM rainfall measurements show a good agreement with limited observational  
351 precipitation records (Awange et al., 2008; Awange et al., 2014).

352

353

## 354 **3.2 Methodologies**

### 355 **3.2.1 GRACE $\Delta$ TWS estimation**

356 First, the  $1^\circ \times 1^\circ$  gridded monthly anomalies of GRACE-derived  $\Delta$ TWS and GLDAS LSMs  
357 derived  $\Delta$ SMS are masked over the area of LVB and LKB (see supplementary Fig. S1). GRACE  
358  $\Delta$ TWS along with GLDAS  $\Delta$ SMS are extracted for the marked  $1^\circ \times 1^\circ$  grid cells for LVB and  
359 LKB and the grid values are spatially aggregated to form time-series of monthly anomalies  
360  $\Delta$ TWS and  $\Delta$ SMS. Second, scaling coefficients or factors provided at  $1^\circ \times 1^\circ$  grids are applied to  
361 each corresponding GRACE  $\Delta$ TWS grids for NASA's *GRCTellus* products only in order to  
362 restore attenuated signals during the post-processing using Eq. (4) (Landerer and Swenson,  
363 2012). We apply an ensemble mean GRACE  $\Delta$ TWS of 3 *GRCTellus* gridded products (i.e., CSR,  
364 GFZ, and JPL solutions) as our exploratory analyses reveal that the time-series records over the  
365 Lake Victoria Basin are highly correlated ( $r > 0.95$ ,  $p$ -value  $< 0.001$ ) and the Root Mean Square  
366 Error (RMSE) is very small (ranges from 1.3 to 1.9 cm) among the time-series records.

367

$$368 \quad g^1(x, y, t) = g(x, y, t) \times s(x, y) \quad (4)$$

369

370 Here,  $g^1(x, y, t)$  represents each un-scaled grid where  $x$  represents longitude,  $y$  represents  
371 latitude, and  $t$  represents time (month), and  $s(x, y)$  is the corresponding scaling factor.





372

### 373 **3.2.2 GRACE $\Delta$ TWS reconciliation**

374 Reconciling GRACE-derived TWS with ground-based observations is limited by the paucity of  
375 in situ observations of SMS, SWS and GWS in many environments. In addition, direct  
376 comparisons between in situ observations of  $\Delta$ SMS,  $\Delta$ SWS and  $\Delta$ GWS and gridded GRACE  
377  $\Delta$ TWS anomalies are complicated by substantial differences in spatial scales, which need to be  
378 considered prior to analysis (Becker et al., 2010). The disaggregation of GRACE  $\Delta$ TWS into  
379 individual water store can also propagate errors to disaggregated components. Here, we construct  
380 in situ  $\Delta$ TWS (i.e., combined signals of  $\Delta$ SMS,  $\Delta$ SWS and  $\Delta$ GWS) for the Lake Victoria Basin  
381 and attempt to reconcile with GRACE-derived  $\Delta$ TWS. One feature of GRACE  $\Delta$ TWS among the  
382 3 solutions we apply in this study is the considerable variation in amplitudes that exist over the  
383 period of 2003 to 2012. In addition, for the *GRCTellus* products, we conduct scaling  
384 experiments, outlined below, to both the ensemble GRACE  $\Delta$ TWS and in situ  $\Delta$ SWS in an  
385 attempt to reconcile satellite and in situ measures.

386

387 Firstly, *GRCTellus* GRACE  $\Delta$ TWS gridded data are generally scaled up using dimensionless  
388 gridded scaling factors that are provided separately and are independent of  $\Delta$ TWS grids  
389 (Landerer and Swenson, 2012). A number of GRACE studies (Rodell et al., 2009; Sun et al.,  
390 2010; Shamsudduha et al., 2012) around the world have applied scaling factors in three different  
391 ways: (1) single scaling factor based on regionally averaged time series, (2) spatially distributed  
392 or gridded scaling factors based on time-series at each grid point, and (3) gridded-gain factors  
393 estimated as a function time or of temporal frequency (Landerer and Swenson, 2012; Long et al.,  
394 2015). In this study, we apply the gridded scaling factors approach to adjust  $\Delta$ TWS time-series



395 records. For a further experiment, we apply a basin-averaged scaling factor ranging from 1.1 to  
396 2.0 and employ RMSE to assess their relative performance. With reference to GRACE  $\Delta$ TWS  
397 and in situ  $\Delta$ TWS relationship, the scaling factor producing the lowest RMSE is applied.

398

399 Secondly, in the LVB,  $\Delta$ SWS is the largest contributor to  $\Delta$ TWS. GRACE  $\Delta$ TWS analyses  
400 commonly apply the same scaling factor as  $\Delta$ TWS to all other individual components (Landerer  
401 and Swenson, 2012). We apply spatially-averaged scaling factors representative of (1) Lake  
402 Victoria and its surrounding grid cells (experiment 1:  $s=0.71$ ; range 0.02–1.5), and (2) the open-  
403 water surface of Lake Victoria without surrounding grid cells (experiment 2:  $s=0.11$ ; range  
404 0.02–0.30). In addition, we also apply a spatially-averaged scaling factor ( $s=0.39$ ; range  
405 0.03–1.48) to JLP-Mascons signal to adjust the in-situ  $\Delta$ SWS.

406

407

#### 408 **4. Results**

409 Monthly time-series records (January 2003 to December 2012) are presented in Figures 5 and 6  
410 respectively for Lake Victoria Basin (LVB) and Lake Kyoga Basin (LKB) of (a) GRACE  $\Delta$ TWS  
411 from *GRCTellus* GRACE  $\Delta$ TWS (ensemble mean of CSR, GFZ, and JPL solutions), GRGS and  
412 JPL-Mascons, (b) GLDAS land surface models (LSMs) derived  $\Delta$ SMS (ensemble mean of 3  
413 LSMs: NOAH, CLM, VIC), (c) in situ  $\Delta$ SWS from lake levels records, and (d) in situ  $\Delta$ GWS  
414 borehole observations. Monthly rainfall derived from TRMM satellite observations over the  
415 same period are shown on the bottom panel (d). Time-series records of all  $\Delta$ TWS components  
416 and rainfall are aggregated for LVB to represent the average seasonal (monthly) pattern of each



417 signal (Fig. 4) that shows an obvious lag (~1 month) between peak rainfall (March–April) and  
418  $\Delta$ TWS and its individual components.

419

420 Mean annual (2003–2012) amplitudes of various GRACE-derived  $\Delta$ TWS signals, in situ  $\Delta$ TWS,  
421 ensemble mean of simulated  $\Delta$ SMS, in situ  $\Delta$ SWS and  $\Delta$ GWS time-series records (Figs. 5 and 6)  
422 are calculated (see supplementary Table S1) for both LVB and LKB. Mean annual amplitude of  
423 GRACE  $\Delta$ TWS ranges from 11.7 to 20.6 cm among *GRCTellus*, GRGS and JPL-MASCON  
424 GRACE products in LVB, and from 8.4 to 16.4 respectively in LKB. Mean annual amplitude of  
425 in situ  $\Delta$ SWS is much greater (14.8 cm) in LVB than in LKB (3.8 cm). GLDAS LSMs derived  
426 ensemble mean  $\Delta$ SMS amplitude in LVB is 7.9 cm and 7.3 cm in LKB. The standard deviation  
427 in  $\Delta$ SMS varies substantially in LVB (1.2 cm, 4.2 cm, and 2.9 cm) LKB (1.3 cm, 4.7 cm, and 4.0  
428 cm) for CLM, NOAH, and VIC models respectively. Mean annual amplitude of in situ  $\Delta$ GWS  
429 ranges from 4.4 cm (LVB) to 3.5 cm (LKB).

430

431 Time-series correlation (Pearson) analysis over various periods of interests (decadal: 2003–2012;  
432 well-constrained SWS reduction or a period of unintended experiment: 2003–2006; controlled  
433 dam operation: 2007–2012) reveals that GRACE-derived  $\Delta$ TWS signals are strongly correlated  
434 in both LVB and LKB (see supplementary Figs. S2–S7). For example, in LVB, in situ  $\Delta$ SWS  
435 shows a statistically significant ( $p$ -value  $<0.001$ ) strong correlation ( $r=0.77$ – $0.92$ ) with all  
436 GRACE-  $\Delta$ TWS time-series (2003–2012) records. Similarly, simulated  $\Delta$ SWS shows  
437 statistically significant ( $p$ -value  $<0.001$ ) strong correlation ( $r=0.72$ – $0.78$ ) with  $\Delta$ TWS time-series  
438 records. In contrast, in situ  $\Delta$ GWS shows statistically significant ( $p$ -value  $<0.001$ ) but moderate  
439 correlation ( $r=0.46$ – $0.56$ ) with  $\Delta$ TWS time-series records. Correlation among the variables



440 shows similar statistical associations for the periods of unintended experiment (2003–2006) and  
441 controlled dam operation (2007–2012). In LKB, however, correlation among in situ  $\Delta$ SWS and  
442 GRACE  $\Delta$ TWS time-series records is statistically significant ( $p$ -value  $< 0.001$ ) but poor in  
443 strength ( $r=0.28$ – $0.34$ ). In situ  $\Delta$ GWS shows statistically significant ( $p$ -value  $< 0.001$ ) moderate  
444 correlation ( $r=0.40$ – $0.47$ ) with GRACE  $\Delta$ TWS time-series records.

445

446 Time-series records of all 5 GRACE  $\Delta$ TWS and in situ  $\Delta$ TWS time-series records in both LVB  
447 and LKB are shown in Figure 7 and results of temporal trends are summarised in Table 3.

448 Statistically significant ( $p$ -value  $< 0.05$ ) declining trends ( $-4.1$  to  $-11.0$   $\text{cm yr}^{-1}$  in LVB;  $-2.1$  to  $-$   
449  $5.6$   $\text{cm yr}^{-1}$  in LKB) are consistently observed during the period of 2004 to 2006. Trends are all  
450 positive in GRACE  $\Delta$ TWS and in situ  $\Delta$ TWS time-series records over the recent period of

451 controlled dam operation (2007–2012) in both LVB and LKB. Therefore, the overall, decadal  
452 (2003–2012) trends are slightly rising ( $0.04$  to  $0.79$   $\text{cm yr}^{-1}$ ) in LVB but nearly stable ( $-0.01$   $\text{cm}$   
453  $\text{yr}^{-1}$ ) in *GRCTellus*  $\Delta$ TWS and slightly declining ( $-0.56$   $\text{cm yr}^{-1}$ ) in situ  $\Delta$ TWS over LKB. In

454 addition, short-term volumetric trends (2004–2006) in GRACE and in situ  $\Delta$ TWS as well as  
455 simulated  $\Delta$ SMS and in situ  $\Delta$ SWS are declining whereas in situ  $\Delta$ GWS and rainfall anomalies  
456 show slightly rising trends over the same period in LVB (see supplementary Figs. S8–S9).

457 Similar trends are reported in various signals over LKB but magnitudes are much smaller  
458 compared to that of LVB, which is 3 times larger than LKB. Volumetric declines in  $\Delta$ TWS in the  
459 LVB for the period 2004 to 2006 are:  $75$   $\text{km}^3$  (in situ),  $68$   $\text{km}^3$  (GRGS),  $50$   $\text{km}^3$  (JPL-Mascons),  
460 and  $26$   $\text{km}^3$  (*GRCTellus* ensemble mean of CRS, JPL and GFZ products).

461

462



463 Linear regression reveals that the association between GRACE-derived  $\Delta$ TWS and in situ  $\Delta$ TWS  
464 is stronger in LVB ( $R^2=0.77-0.91$ ) than in LKB ( $R^2=0.49-0.55$ ) (see supplementary Table S1).  
465 GRACE  $\Delta$ TWS is unable to explain natural variability in in situ  $\Delta$ TWS in LKB though this may  
466 be explained by the fact that SWS in Lake Kyoga is influenced by dam releases from LVB.  
467 Multiple linear regression analysis reveals that the relative proportion of variability in in situ  
468  $\Delta$ TWS time-series record can be explained by  $\Delta$ SWS (88.9 %),  $\Delta$ SMS (9.4 %) and  $\Delta$ GWS (1.9  
469 %) in LVB; and by 37.2 %, 55.9 % and 6.9 % respectively in LKB. These results are indicative  
470 only as these percentages can be biased by the presence of strong correlation among variables  
471 and the order of these variables listed as predictors in the regression model.

472

473 Disaggregation of  $\Delta$ GWS from GRACE  $\Delta$ TWS time-series record from each product has been  
474 carefully considered. In case of LVB, we apply a spatially-averaged multiplicative scaling factor  
475 (1.7) to *GRCTellus* GRACE-derived  $\Delta$ TWS dataset to amplify the signal that is better reconciled  
476 with in situ  $\Delta$ TWS (see supplementary Fig. S10). Additionally, for both *GRCTellus* and JPL-  
477 Mascons  $\Delta$ TWS disaggregation to  $\Delta$ GWS a scaled down signal of in situ  $\Delta$ SWS is applied.  
478 Time-series record (2003–2012) of in situ  $\Delta$ GWS in LVB weakly correlates ( $r=0.29$ ,  $p$ -value  
479  $<0.001$ ) with both *GRCTellus* and JPL-Mascons GRACE derived  $\Delta$ GWS but shows no  
480 correlation with GRGS  $\Delta$ GWS (Fig. 8).

481

482 In LKB, in situ  $\Delta$ GWS time-series record shows weaker and statistically insignificant correlation  
483 ( $r=0.16-0.19$ ,  $p$ -value  $<0.08$ ) with JPL-Mascons and GRGS GRACE-derived  $\Delta$ GWS but shows  
484 no correlation with *GRCTellus*  $\Delta$ GWS (see supplementary Fig. S11). Furthermore, RMSE  
485 among various GRACE-derived estimates of  $\Delta$ GWS and in situ  $\Delta$ GWS ranges from 3.0 cm



486 (GRACE ensemble), 3.7 cm (GRGS) to 6.4 cm (JPL-Mascons) in LVB, and from 3.4 (GRACE  
487 ensemble), 5.6 cm (GRGS) to 6.8 cm (JPL-Mascons) in LKB.

488

## 489 5. Discussion

490 We apply 5 different gridded GRACE products (*GRCTellus* – CSR, JPL and GFZ; GRGS and  
491 JPL-Mascons) to test  $\Delta$ TWS signals for in the Lake Victoria Basin (LVB) comprising a large and  
492 accurately observed reduction (75 km<sup>3</sup>) in  $\Delta$ TWS from 2004 to 2006. Our analysis reveals that  
493 all GRACE products capture this substantial reduction in terrestrial water mass but the  
494 magnitude of GRACE  $\Delta$ TWS among GRACE products varies substantially. For example,  
495 *GRCTellus* underrepresents greatly (66 %) the reduction in in situ  $\Delta$ TWS whereas GRGS  
496 GRACE product underrepresents slightly (10 %). Over a longer period (2003–2012) in the  
497 Upper Nile Basin, all GRACE products correlate well with in situ  $\Delta$ TWS but, similar to the  
498 unintended experiment, variability in amplitude is considerable (Fig. 9). The average amplitude  
499 of  $\Delta$ TWS is substantially dampened (i.e., 86 % less than in situ  $\Delta$ TWS) in *GRCTellus* GRACE  
500 products relative to GRGS (6 %) and JPL-Mascons (7 %) products in the LVB.

501

502 The ‘true’ amplitude in *GRCTellus*  $\Delta$ TWS signal is generally reduced during the post-processing  
503 of GRACE spherical harmonic fields, primarily due to spatial smoothing by a large-scale (e.g.,  
504 300 km) Gaussian filter and truncation of gravity fields at a higher (degree 60 = 300 km) spectral  
505 degree (Swenson and Wahr, 2006; Landerer and Swenson, 2012). Despite the application of  
506 scaling coefficients based on CLM v.4.0 to amplify *GRCTellus*  $\Delta$ TWS amplitudes at individual  
507 grids, the basin-averaged (LVB) time-series record represents only 77 % variability in in situ



508  $\Delta$ TWS. Scaling experiments conducted here reveal that *GRCTellus*  $\Delta$ TWS requires an additional  
509 multiplicative factor of 1.7 in order to match in situ  $\Delta$ TWS with a minimum RMSE (5.8 cm). On  
510 the other hand, NASA's new gridded GRACE product, JPL-Mascons, that applies a priori  
511 constraint in space and time to derive monthly gravity fields and undergoes some degree of  
512 spatial smoothing (Watkins et al., 2015), represents nearly 85 % variability in in-situ  $\Delta$ TWS. In  
513 contrast, GRGS GRACE product, although applying truncation at degree 80 (~250 km), does not  
514 suffer from any large-scale spatial smoothing and, is able to represent well (92 %) the variability  
515 in in situ  $\Delta$ TWS in the LVB.

516

517 A priori corrections of *GRCTellus* ensemble mean GRACE signals using a set of LSM-derived  
518 scaling factors (i.e., amplitude gain) can lead to substantial uncertainty in  $\Delta$ TWS (Long et al.,  
519 2015). We show that the amplitude of simulated terrestrial water mass over the Upper Nile  
520 Basins varies substantially among various LSMs (see supplementary Fig. S12). Most of these  
521 LSMs (GLDAS models: CLM, NOAH, VIC) do not include surface water or groundwater  
522 storage (Scanlon et al., 2012). Although CLM (v.4.0 and 4.5) includes a simple representation  
523 (i.e., shallow unconfined aquifer) of groundwater (Niu et al., 2007; Oleson et al., 2008), it does  
524 not consider recharge from irrigation return flows. In addition, many of these LSMs do not  
525 consider lakes and reservoirs and, most critically, LSMs are not reconciled with in situ  
526 observations. As a result, methods of rescaling the amplitude of GRACE signals based on a  
527 priori information from LSMs contribute uncertainty to TWS signals.

528

529 The combined measurement and leakage errors,  $\sqrt{(bias^2 + leak^2)}$  (Swenson and Wahr, 2006)  
530 for *GRCTellus*  $\Delta$ TWS based on CLM4.0 model for LVB and LKB are 7.2 cm and 6.6 cm



531 respectively. These values, however, do not represent mass leakage from the lake to the  
532 surrounding area within the basin itself. A sensitivity analysis of *GRCTellus* and GRGS signals  
533 for leakage from the lake into the basin area shows that leakage from Lake Victoria to LVB for  
534 *GRCTellus* is substantially greater than GRGS product by a factor of ~2.6. In other words, 1 mm  
535 change in the level of Lake Victoria represents an equivalent change of 0.12 mm in  $\Delta$ TWS in  
536 LVB for *GRCTellus* compared to 0.32 mm for GRGS. Consequently, changes in the amplitude  
537 of GRGS  $\Delta$ TWS are much greater (~38 %) than *GRCTellus*. During the observed reduction in  
538  $\Delta$ TWS (75 km<sup>3</sup>) from 2004 to 2006, the computed amplitude for GRGS is 68 km<sup>3</sup> whereas it is  
539 26 km<sup>3</sup> for *GRCTellus*.

540

541 Another source of uncertainty that contributes toward  $\Delta$ TWS anomalies in GRACE analysis is  
542 the choice of simulated  $\Delta$ SMS from various global-scale LSMs (e.g., Shamsudduha et al., 2012;  
543 Scanlon et al., 2015). For example, the mean annual (2003–2012) amplitudes in simulated  $\Delta$ SMS  
544 in GLDAS LSMs (CLM, NOAH, VIC) vary substantially in LVB (3.5 cm, 10.2 cm, and 10.5  
545 cm) and LKB (3.7 cm, 10.6 cm, and 7.7 cm) respectively. Due to an absence of a dedicated  
546 monitoring network for soil moisture in the Upper Nile Basin, this study like many other  
547 GRACE studies, is resigned to applying simulated  $\Delta$ SMS from multiple LSMs arguing that the  
548 use of an ensemble mean minimises the error associated with  $\Delta$ SMS (Rodell et al., 2009).

549

550 Computed contributions of  $\Delta$ GWS to  $\Delta$ TWS in the Upper Nile Basins are low (<10 %).  
551 GRACE-derived estimates of  $\Delta$ GWS from all three products (*GRCTellus*, GRGS and JPL-  
552 Mascons) correlate very weakly with in situ  $\Delta$ GWS in both LVB and LKB. One curious  
553 observation in LVB during the unintended experiment (2005–2006) is that in situ  $\Delta$ GWS rises





554 whereas in situ  $\Delta$ SWS and simulated  $\Delta$ SMS decline. The available evidence in groundwater-  
555 level records (e.g., Entebbe, Uganda) suggests that rainfall-generated groundwater recharge led  
556 to an increased in  $\Delta$ GWS while dam releases exceeding the “Agreed Curve” continued to reduce  
557  $\Delta$ SWS (Owor et al., 2011).

558

559 Uncertainties in the estimation of GRACE-derived  $\Delta$ GWS remain in: (i) the choice of scaling  
560 factors applied to in situ  $\Delta$ SWS associated with the disaggregation of  $\Delta$ TWS from JPL-Mascons  
561 and *GRCTellus* GRACE products, (ii) simulated  $\Delta$ SMS by GLDAS land surface models, (iii) the  
562 very limited spatial coverage in piezometry to represent in situ  $\Delta$ GWS, and (iv) applied  $S_y$  (3 %  
563 with range from 1 % to 6 %) to convert in situ groundwater levels to  $\Delta$ GWS. The lack of any  
564 correlation in GRGS and in situ  $\Delta$ GWS time-series records indicates that the magnitude of  
565 uncertainty is larger than the overall variability in  $\Delta$ GWS in low-storage, low-transmissivity  
566 weathered crystalline aquifers within the Upper Nile Basin. In contrast to the assertions of  
567 Nanteza et al. (2016) applying the *GRCTellus* CSR solution, we find that this uncertainty  
568 prevents robust resolution of  $\Delta$ GWS from GRACE  $\Delta$ TWS in these complex hydrogeological  
569 environments of East Africa. Despite substantial efforts to improve groundwater-level  
570 monitoring<sup>1</sup> and to collate existing groundwater-level records<sup>2</sup> across Africa, we recognise that  
571 understanding of in situ  $\Delta$ GWS remains greatly constrained by limitations in current  
572 observational networks and records. Since present uncertainties and limitations identified in the  
573 Upper Nile Basin occur in many of the weathered hard-rock aquifer environments that underlie  
574 40% of Sub-Saharan Africa (MacDonald et al., 2012), tracing of  $\Delta$ GWS using GRACE in these  
575 areas is unlikely to be robust until these uncertainties and limitations are better constrained.

<sup>1</sup> UPGro programme: <https://upgro.org/>

<sup>2</sup> The Chronicles Consortium: <https://www.un-igrac.org/special-project/chronicles-consortium>



576 **6. Conclusions**

577 The analysis of a large, accurately recorded reduction in the volume of Lake Victoria ( $\Delta\text{SWS}=81$   
578  $\text{km}^3$ ) from 2004 to 2006 exposes substantial variability among commonly-used 5 gridded  
579 GRACE products (*GRCTellus* CSR, JPL, GFZ; GRGS; JPL-Mascons) to quantify the amplitude  
580 of changes in terrestrial water storage ( $\Delta\text{TWS}$ ). For this event, we estimate an overall decline in  
581 'in situ'  $\Delta\text{TWS}$  (i.e., in situ  $\Delta\text{SWS}$  and  $\Delta\text{GWS}$ ; simulated  $\Delta\text{SMS}$ ) over the Lake Victoria Basin  
582 (LVB) of  $75 \text{ km}^3$ . This value compares favourably with GRGS GRACE  $\Delta\text{TWS}$  ( $68 \text{ km}^3$ ), is  
583 underrepresented by JPL-Mascons GRACE  $\Delta\text{TWS}$  ( $50 \text{ km}^3$ ), and is substantially  
584 underrepresented by the ensemble mean of *GRCTellus* GRACE  $\Delta\text{TWS}$  ( $26 \text{ km}^3$ ). Attempts to  
585 better reconcile *GRCTellus* GRACE  $\Delta\text{TWS}$  to in situ  $\Delta\text{TWS}$  through scaling techniques are  
586 unable to represent adequately the observed amplitude in  $\Delta\text{TWS}$ .

587

588 From 2003 to 2012, GRGS, JPL-Mascons and *GRCTellus* GRACE products trace well the phase  
589 in in situ  $\Delta\text{TWS}$  in the Upper Nile Basin that comprises both the LVB and Lake Kyoga Basin  
590 (LKB). In the LVB for example, each explains 91 % (GRGS), 85 % (JPL-Mascons), and 77 %  
591 (*GRCTellus* ensemble mean of CSR, JPL and GFZ) of the variance, respectively, in in situ  
592  $\Delta\text{TWS}$ . The relative proportion of variability in in situ  $\Delta\text{TWS}$  (variance  $120 \text{ cm}^2$  LVB,  $24 \text{ cm}^2$   
593 LKB) is explained by in situ  $\Delta\text{SWS}$  (89 % LVB; 37 % LKB), GLDAS ensemble mean  $\Delta\text{SMS}$  (9  
594 % LVB; 56 % LKB) and in situ  $\Delta\text{GWS}$  (2 % LVB; 7 % LKB); these percentages are indicative  
595 as individual TWS components are strongly correlated. In situ  $\Delta\text{GWS}$  contributes minimally to  
596  $\Delta\text{TWS}$  and is only moderately associated with  $\Delta\text{TWS}$  ( $r=0.57$ ,  $p$ -value  $<0.001$ ). Resolution of  
597  $\Delta\text{GWS}$  from GRACE  $\Delta\text{TWS}$  in the Upper Nile Basin relies upon robust measures of  $\Delta\text{SWS}$  and  
598  $\Delta\text{SMS}$ ; the former is observed in situ whereas the latter is limited by uncertainty in simulated



599  $\Delta$ SMS, represented here and in many GRACE studies by an ensemble mean of GLDAS LSMs.  
600 Mean annual amplitudes in observed  $\Delta$ GWS (2003–2012) from limited piezometry for the low-  
601 storage and low-transmissivity aquifers in deeply weathered crystalline rocks that underlie the  
602 Upper Nile Basin are small (3.5 to 4.4 cm for  $S_y=0.03$ ) and, given the current uncertainty in  
603 simulated  $\Delta$ SMS, are beyond the limit of what can be reliably quantified using current GRACE  
604 satellite products.  
605  
606 Our examination of a large, mass-storage change (2004 to 2006) observed in the Lake Victoria  
607 Basin highlights substantial variability in the measurement of  $\Delta$ TWS using different gridded  
608 GRACE products. Although the phase in  $\Delta$ TWS is generally well recorded by all tested GRACE  
609 products, substantial differences exist in the amplitude of  $\Delta$ TWS that also influence the  
610 disaggregation of individual terrestrial stores (e.g., groundwater storage) and estimation of trends  
611 in TWS and individual, disaggregated freshwater stores. We note that the stronger filtering of the  
612 large-scale (~300 km) gravity signal associated with *GRCTellus* results in greater signal leakage  
613 relative to GRGS and JPL-Mascons. As a result, greater rescaling is required to resurrect signal  
614 amplitudes in *GRCTellus* relative to GRGS and JPL-Mascons and these scaling factors depend  
615 upon uncertain and incomplete a priori knowledge of terrestrial water stores derived from large-  
616 scale models, which generally do not consider the existence of Lake Victoria, the second largest  
617 lake by area in the world.  
618



619 **Author contribution**

620 RT conceived this study for which preliminary analyses were carried out by DJ and MS. MS and  
621 DJ have processed GRACE and all observational datasets and conducted statistical analyses and  
622 GIS mapping. LL conducted the analysis of spatial leakage and bias in GRACE signals. CT, RT  
623 and MO helped to establish, collate and analyse groundwater-level data; CT provided dam  
624 release data. MS and RT wrote the manuscript and LL, DJ, MO and CT commented on draft  
625 manuscripts.

626

627 **Competing interests**

628 The authors declare that they have no conflict of interest.

629

630 **Acknowledgements**

631 We kindly acknowledge NASA's MEaSURES Program (<http://grace.jpl.nasa.gov>) for the freely  
632 available gridded *GRCTellus* and JPL-MASCON GRACE data and French National Centre for  
633 Space Studies (CNES) for GRGS GRACE data. NASA's Precipitation Processing Centre and  
634 NASA's Hydrological Sciences Laboratory and the Goddard Earth Sciences Data and  
635 Information Services Centre (GES DISC) are duly acknowledged for TRMM rainfall and soil  
636 moisture data from GLDAS Land Surface Models. We kindly acknowledge the Directorate of  
637 Water Resources Management in the Ministry of Water and Environment (Uganda) for the  
638 provision of piezometric and lake-level data. Support from the UK government's UPGro  
639 Programme, funded by the Natural Environment Research Council (NERC), Economic and  
640 Social Research Council (ESRC) and the Department For International Development (DFID)  
641 through the *GroFutures: Groundwater Futures in Sub-Saharan Africa* catalyst NE/L002043/1)  
642 and consortium (NE/M008932/1) grant awards, is gratefully acknowledged.



643 **References**

644

- 645 Arendt, A. A., Luthcke, S. B., Gardner, A. S., O'Neel, S., Hill, D., Moholdt, G., and Abdalati,  
646 W.: Analysis of a GRACE global mascon solution for Gulf of Alaska glaciers, *Journal of*  
647 *Glaciology*, 59, 913-924, doi:10.3189/2013JoG12J197, 2013.
- 648 Awange, J. L., Sharifi, M. A., Ogonda, G., Wickert, J., Grafarend, E., and Omulo, M.: The  
649 falling Lake Victoria water levels: GRACE, TRIMM and CHAMP satellite analysis of the  
650 lake basin, *Water Resources Management*, 22, 775-796, 2008.
- 651 Awange, J. L., Anyah, R., Agola, N., Forootan, E., and Omondi, P.: Potential impacts of climate  
652 and environmental change on the stored water of Lake Victoria Basin and economic  
653 implications, *Water Resour. Res.*, 49, 8160-8173, 2013.
- 654 Awange, J. L., Forootan, E., Kuhn, M., Kusche, J., and Heck, B.: Water storage changes and  
655 climate variability within the Nile Basin between 2002 and 2011, *Advances in Water*  
656 *Resources*, 73, 1-15, 2014.
- 657 Basalirwa, C. P. K.: Delineation of Uganda into climatological rainfall zones using the method of  
658 Principle Component Analysis, *International Journal of Climatology*, 15, 1161-1177, 1995.
- 659 Becker, M., Llovel, W., Cazenave, A., Güntner, A., and Crétaux, J.-F.: Recent hydrological  
660 behaviour of the East African great lakes region inferred from GRACE, satellite altimetry  
661 and rainfall observations, *Comptes Rendus Geoscience*, 342, 223-233, 2010.
- 662 Biancale, R., Lemoine, J.-M., Balmino, G., Loyer, S., Bruisma, S., Perosanz, F., Marty, J.-C.,  
663 and Gégout, P.: 3 Years of Geoid Variations from GRACE and LAGEOS Data at 10-day  
664 Intervals from July 2002 to March 2005, CNES/GRGS, 2006.
- 665 Brown, E., and Sutcliffe, J. V.: The water balance of Lake Kyoga, Uganda, *Hydrological*  
666 *Sciences Journal*, 58, 342-353, doi: 10.1080/02626667.2012.753148, 2013.
- 667 Bruinsma, S., Lemoine, J.-M., and Biancale, R.: CNES/GRGS 10-day gravity field models  
668 (release 2) and their evaluation *Adv. Space Res.*, 45, 587-601, 10.1016/j.asr.2009.10.012,  
669 2010.



- 670 Castellazzi, P., Martel, R., Galloway, D. L., Longuevergne, L., and Rivera, A.: Assessing  
671 Groundwater Depletion and Dynamics Using GRACE and InSAR: Potential and  
672 Limitations, *Ground Water*, doi:10.1111/gwat.12453, 2016.
- 673 Chen, J. L., Wilson, C. R., and Tapley, B. D.: The 2009 exceptional Amazon flood and  
674 interannual terrestrial water storage change observed by GRACE, *Water Resour. Res.*, 46,  
675 W12526, 2010.
- 676 GRACE (Gravity Recovery and Climate Experiment) (<http://www.csr.utexas.edu/grace/>), access:  
677 03 August, 2016.
- 678 Dai, Y., Zeng, X., Dickinson, R. E., Baker, I., Bonan, G. B., Bosilovich, M. G., Denning, A. S.,  
679 Dirmeyer, P. A., Houser, P. R., Niu, G., Oleson, K. W., Schlosser, C. A., and Yang, Z.-L.:  
680 The common land model (CLM), *Bull. Am. Meteorol. Soc.*, 84, 1013-1023, 2003.
- 681 Ek, M. B., Mitchell, K. E., Lin, Y., Rogers, E., Grunmann, P., Koren, V., Gayno, G., and  
682 Tarpley, J. D.: Implementation of Noah land surface model advances in the National Centers  
683 for Environmental Prediction operational mesoscale Eta model, *J. Geophys. Res.*, 108(D22),  
684 8851, 10.1029/2002JD003296, 2003.
- 685 Famiglietti, J. S., Lo, M., Ho, S. L., Bethune, J., Anderson, K. J., Syed, T. H., Swenson, S. C.,  
686 Linage, C. R. d., and Rodell, M.: Satellites measure recent rates of groundwater depletion in  
687 California's Central Valley, *Geophys. Res. Lett.*, 38, L03403, 10.1029/2010GL046442,  
688 2011.
- 689 Frappart, F., Ramillien, G., and Famiglietti, J. S.: Water balance of the Arctic drainage system  
690 using GRACE gravimetry products, *International Journal of Remote Sensing*, 32, 431-453,  
691 doi:10.1080/01431160903474954, 2011.
- 692 Geruo, A., Wahr, J., and Zhong, S.: Computations of the viscoelastic response of a 3-D  
693 compressible Earth to surface loading: an application to Glacial Isostatic Adjustment in  
694 Antarctica and Canada, *Geophys. J. Int.*, 192, 557-572, 2013.
- 695 Güntner, A.: Improvement of Global Hydrological Models Using GRACE Data, *Surveys in*  
696 *Geophysics*, 29, 375-397, 2008.



- 697 Hoogeveen, J., Faurès, J.-M., Peiser, L., Burke, J., and Giesen, N. v. d.: GlobWat – a global  
698 water balance model to assess water use in irrigated agriculture, *Hydrol. Earth Syst. Sci.*, 19,  
699 3829-3844, 2015.
- 700 Hu, L., and Jiao, J. J.: Calibration of a large-scale groundwater flow model using GRACE data: a  
701 case study in the Qaidam Basin, China, *Hydrogeol. J.*, 23, 1305-1317, 2015.
- 702 Huffman, G. J., Adler, R. F., Bolvin, D. T., Gu, G., Nelkin, E. J., Bowman, K. P., Hong, Y.,  
703 Stocker, E. F., and Wolff, D. B.: The TRMM multi-satellite precipitation analysis: quasi-  
704 global, multi-year, combined-sensor precipitation estimates at fine scale, *J. Hydrometeorol.*,  
705 8 (1), 38-55, 2007.
- 706 Humphrey, V., Gudmundsson, L., and Seneviratne, S. I.: Assessing Global Water Storage  
707 Variability from GRACE: Trends, Seasonal Cycle, Subseasonal Anomalies and Extremes,  
708 *Surveys in Geophysics*, 37, 357-395, doi:10.1007/s10712-016-9367-1, 2016.
- 709 Indeje, M., Semazzi, F. H. M., and Ogallo, L. J.: ENSO signals in East African rainfall seasons,  
710 *International Journal of Climatology*, 20, 19-46, 2000.
- 711 Jacob, T., Wahr, J., Pfeffer, W. T., and Swenson, S.: Recent contributions of glaciers and ice  
712 caps to sea level rise, *Nature*, 482, 514-518, 2012.
- 713 Jiang, D., Wang, J., Huang, Y., Zhou, K., Ding, X., and Fu, J.: The Review of GRACE Data  
714 Applications in Terrestrial Hydrology Monitoring, *Advances in Meteorology*, Article ID  
715 725131, 2014.
- 716 Khandu, Forootan, E., Schumacher, M., Awange, J. L., and Schmied, H. M.: Exploring the  
717 influence of precipitation extremes and humanwater use on total water storage  
718 (TWS)changes in the Ganges-Brahmaputra-Meghna River Basin, *Water Resour. Res.*, 52,  
719 2240-2258, doi:10.1002/2015WR018113, 2016.
- 720 Kim, H., Yeh, P. J.-F., Oki, T., and Kanae, S.: Role of rivers in the seasonal variations of  
721 terrestrial water storage over global basins, *Geophys. Res. Lett.*, 36, L17402,  
722 doi:10.1029/2009GL039006, 2009.
- 723 Kizza, M., Westerberg, I., Rodhe, A., and Ntale, H.: Estimating areal rainfall over Lake Victoria  
724 and its basin using ground-based and satellite data, *Journal of Hydrology*, 464-465, 401-411,  
725 2012.



- 726 Krishnamurthy, K. V., and Ibrahim, A. M.: Hydrometeorological Studies of Lakes Victoria,  
727 Kyoga, and Albert, in: Unintended Lakes: Their Problems and Environmental Effects, edited  
728 by: Ackermann, W. C., White, G. F., Worthington, E. B., and Ivens, J. L., American  
729 Geophysical Union, Washington D.C., 2013.
- 730 Kusche, J., Eicker, A., Forootan, E., Springer, A., and Longuevergne, L.: Mapping probabilities  
731 of extreme continental water storage changes from space gravimetry, *Geophys. Res. Lett.*,  
732 43, 8026-8034, doi:10.1002/2016GL069538, 2016.
- 733 Landerer, F. W., and Swenson, S. C.: Accuracy of scaled GRACE terrestrial water storage  
734 estimates, *Water Resour. Res.*, 48, W04531, 2012.
- 735 Leblanc, M. J., Tregoning, P., Ramillien, G., Tweed, S. O., and Fakes, A.: Basin-scale,  
736 integrated observations of the early 21st century multiyear drought in southeast Australia,  
737 *Water Resour. Res.*, 45, W04408, doi:10.1029/2008WR007333, 2009.
- 738 Lehner, B., Verdin, K., and Jarvis, A.: HydroSHEDS technical documentation, World Wildlife  
739 Fund, Washington D.C., 2006.
- 740 Lehner, B., Verdin, K., and Jarvis, A.: New global hydrography derived from spaceborne  
741 elevation data, *Eos, Transactions American Geophysical Union*, 89, 93-94, 2008.
- 742 Lemoine, J.-M., Bruisma, S., Loyer, S., Biancale, R., Marty, J.-C., Perosanz, F., and Balmino,  
743 G.: Temporal gravity field models inferred from GRACE data, *Adv. Space Res.*, 39, 1620-  
744 1629, doi: 10.1016/j.asr.2007.03.062, 2007.
- 745 Liang, X., Xie, Z., and Huang, M.: A new parameterization for surface and groundwater  
746 interactions and its impact on water budgets with the variable infiltration capacity (VIC)  
747 land surface model, *J. Geophys. Res.*, 108(D16), 8613, 10.1029/2002JD003090, 2003.
- 748 Long, D., Longuevergne, L., and Scanlon, B. R.: Global analysis of approaches for deriving total  
749 waterstorage changes from GRACE satellites, *Water Resour. Res.*, 51, 2574–2594,  
750 doi:10.1002/2014WR016853, 2015.
- 751 Long, D., Chen, X., Scanlon, B. R., Wada, Y., Hong, Y., Singh, V. P., Chen, Y., Wang, C., Han,  
752 Z., and Yang, W.: Have GRACE satellites overestimated groundwater depletion in the  
753 Northwest India Aquifer?, *Nature Scientific Reports*, 6, 24398, doi:10.1038/srep24398,  
754 2016.





- 755 Longuevergne, L., Scanlon, B. R., and Wilson, C. R.: GRACE hydrological estimates for small  
756 basins: evaluating processing approaches on the High Plains Aquifer, USA, *Water Resour.*  
757 *Res.*, 46, W11517, 2010.
- 758 Longuevergne, L., Wilson, C. R., Scanlon, B. R., and Crétaux, J. F.: GRACE water storage  
759 estimates for the Middle East and other regions with significant reservoir and lake storage,  
760 *Hydrol. Earth Syst. Sci.*, 17, 4817-4830, doi:10.5194/hess-17-4817-2013, 2013.
- 761 MacDonald, A. M., Bonsor, H. C., Dochartaigh, B. E. O., and Taylor, R. G.: Quantitative maps  
762 of groundwater resources in Africa, *Environ. Res. Lett.*, 7, doi:10.1088/1748-  
763 9326/1087/1082/024009, 2012.
- 764 Nanteza, J., de Linage, C. R., Thomas, B. F., and Famiglietti, J. S.: Monitoring groundwater  
765 storage changes in complex basement aquifers: An evaluation of the GRACE satellites over  
766 East Africa, *Water Resour. Res.*, 52, doi:10.1002/2016WR018846, 2016.
- 767 Nicholson, S. E., Yin, X., and Ba, M. B.: On the feasibility of using a lake water balance model  
768 to infer rainfall: an example from Lake Victoria, *Hydrological Science Journal*, 45, 75-95,  
769 2000.
- 770 Niu, G.-Y., Yang, Z.-L., Dickinson, R. E., Gulden, L. E., and Su, H.: Development of a simple  
771 groundwater model for use in climate models and evaluation with Gravity Recovery and  
772 Climate Experiment data, *J. Geophys. Res.*, 112, D07103, doi:10.1029/2006JD007522,  
773 2007.
- 774 Oleson, K. W., Niu, G.-Y., Yang, Z.-L., Lawrence, D. M., Thornton, P. E., Lawrence, P. J.,  
775 Stockli, R., Dickinson, R. E., Bonan, G. B., Levis, S., Dai, A., and Qian, T.: Improvements  
776 to the Community Land Model and their impact on the hydrological cycle, *J. Geophys. Res.*,  
777 113, G01021, doi:10.1029/2007JG000563, 2008.
- 778 Owor, M., Taylor, R. G., Tindimugaya, C., and Mwesigwa, D.: Rainfall intensity and  
779 groundwater recharge: empirical evidence from the Upper Nile Basin, *Environmental*  
780 *Research Letters*, 1-6, 2009.
- 781 Owor, M.: Groundwater - surface water interactions on deeply weathered surfaces of low relief  
782 in the Upper Nile Basin of Uganda, Ph.D., Geography, University College London, London,  
783 271 pp., 2010.



- 784 Owor, M., Taylor, R. G., Mukwaya, C., and Tindimugaya, C.: Groundwater/surface-water  
785 interactions on deeply weathered surfaces of low relief: evidence from Lakes Victoria and  
786 Kyoga, Uganda, *Hydrogeol. J.*, 19, 1403-1420, 2011.
- 787 Ramillien, G., Famiglietti, J. S., and Wahr, J.: Detection of Continental Hydrology and  
788 Glaciology Signals from GRACE: A Review, *Surv. Geophys.*, 29, 361-374, 2008.
- 789 Rodell, M., and Famiglietti, J. S.: Terrestrial Water Storage Variations over Illinois: Analysis of  
790 Observations and Implications for GRACE, *Wat. Resour. Res.*, 37, 1327-1340, 2001.
- 791 Rodell, M., Houser, P. R., Jambor, U., Gottschalck, J., Mitchell, K., Meng, C.-J., Arsenault, K.,  
792 Cosgrove, B., Radakovich, J., Bosilovich, M., Entin, J. K., Walker, J. P., Lohmann, D., and  
793 Toll, D.: The Global Land Data Assimilation System, *Bull. Am. Meteorol. Soc.*, 85, 381-  
794 394, 2004.
- 795 Rodell, M., Velicogna, I., and Famiglietti, J. S.: Satellite-based estimates of groundwater  
796 depletion in India, *Nature*, 460, 999-1003, doi:10.1038/nature08238, 2009.
- 797 Rowlands, D. D., Luthcke, S. B., McCarthy, J. J., Klosko, S. M., Chinn, D. S., Lemoine, F. G.,  
798 Boy, J.-P., and Sabaka, T. J.: Global mass flux solutions from GRACE: A comparison of  
799 parameter estimation strategies-Mass concentrations versus stokes coefficients, *J. Geophys.*  
800 *Res.*, 115, B01403, doi:10.1029/2009JB006546, 2010.
- 801 Scanlon, B. R., Longuevergne, L., and Long, D.: Ground referencing GRACE satellite estimates  
802 of groundwater storage changes in the California Central Valley, USA, *Water Resour. Res.*,  
803 48, W04520, 2012.
- 804 Scanlon, B. R., Zhang, Z., Reedy, R. C., Pool, D. R., Save, H., Long, D., Chen, J., Wolock, D.  
805 M., Conway, B. D., and Winester, D.: Hydrologic implications of GRACE satellite data in  
806 the Colorado River Basin, *Water Resour. Res.*, 51, 9891-9903,  
807 doi:10.1002/2015WR018090, 2015.
- 808 Sene, K. J., and Plinston, D. T.: A review and update of the hydrology of Lake Victoria in East  
809 Africa, *Hydrological Sciences Journal*, 39, 47-63, 1994.
- 810 Shamsudduha, M., Taylor, R. G., and Longuevergne, L.: Monitoring groundwater storage  
811 changes in the highly seasonal humid tropics: validation of GRACE measurements in the  
812 Bengal Basin, *Water Resour. Res.*, 48, W02508, doi:10.1029/2011WR010993, 2012.



- 813 Strassberg, G., Scanlon, B. R., and Rodell, M.: Comparison of seasonal terrestrial water storage  
814 variations from GRACE with groundwater-level measurements from the High Plains  
815 Aquifer (USA), *Geophys. Res. Lett.*, 34, L14402, 10.1029/2007GL030139, 2007.
- 816 Sun, A. Y., Green, R., Rodell, M., and Swenson, S.: Inferring aquifer storage parameters using  
817 satellite and in situ measurements: Estimation under uncertainty, *Geophys. Res. Lett.*, 37,  
818 L10401, 10.1029/2010GL043231, 2010.
- 819 Sutcliffe, J. V., and Petersen, G.: Lake Victoria: derivation of a corrected natural water level  
820 series, *Hydrological Sciences Journal*, 52, 1316-1321, 2007.
- 821 Swenson, S., and Wahr, J.: Post-processing removal of correlated errors in GRACE data,  
822 *Geophys. Res. Lett.*, 33, L08402, doi:10.1029/2005GL025285, 2006.
- 823 Tapley, B. D., Bettadpur, S., Ries, J. C., Thompson, P. F., and Watkins, M. M.: GRACE  
824 measurements of mass variability in the Earth system, *Science*, 305, 503-505, 2004.
- 825 Taylor, R., Tindimugaya, C., Barker, J., MacDonald, D., and Kulabako, R.: Convergent radial  
826 tracing of viral and solute transport in gneiss saprolite, *Ground Water*, 48, 284-294, 2010.
- 827 Taylor, R. G., and Howard, K. W. F.: A tectonic geomorphic model of the hydrogeology of  
828 deeply weathered crystalline rock: evidence from Uganda, *Hydrogeol. J.*, 8, 279-294, 2000.
- 829 Taylor, R. G., Todd, M. C., Kongola, L., Maurice, L., Nahozya, E., Sanga, H., and MacDonald,  
830 A. M.: Evidence of the dependence of groundwater resources on extreme rainfall in East  
831 Africa, *Nature Climate Change*, 3, 374-378, doi:10.1038/nclimate1731, 2013.
- 832 UNEP: Adaptation to Climate-change Induced Water Stress in the Nile Basin: A Vulnerability  
833 Assessment Report, Division of Early Warning and Assessment (DEWA). United Nations  
834 Environment Programme (UNEP), Nairobi, Kenya, 2013.
- 835 Vishwakarma, B. D., Devaraju, B., and Sneeuw, N.: Minimizing the effects of filtering on  
836 catchment scale GRACE solutions, *Water Resour. Res.*, 52, 5868-5890,  
837 doi:10.1002/2016WR018960, 2016.
- 838 Vouillamoz, J. M., Lawson, F. M. A., Yalo, N., and Desclotres, M.: The use of magnetic  
839 resonance sounding for quantifying specific yield and transmissivity in hard rock aquifers:  
840 The example of Benin, *Journal of Applied Geophysics*, 107, 16-24, 2014.



- 841 Wahr, J., Swenson, S., Zlotnicki, V., and Velicogna, I.: Time-variable gravity from GRACE:  
842 First results, *Geophys. Res. Lett.*, 31, L11501, doi:10.1029/2004GL019779, 2004.
- 843 Wahr, J., Swenson, S., and Velicogna, I.: Accuracy of GRACE mass estimates, *Geophys. Res.*  
844 *Lett.*, 33, L06401, doi:10.1029/2005GL025305, 2006.
- 845 Wang, L., Davis, J. L., Hill, E. M., and Tamisiea, M. E.: Stochastic filtering for determining  
846 gravity variations for decade-long timeseries of GRACE gravity, *J. Geophys. Res. Solid*  
847 *Earth*, 121, 2915-2931, doi:10.1002/2015JB012650, 2016.
- 848 Watkins, M. M., Wiese, D. N., Yuan, D.-N., Boening, C., and Landerer, F. W.: Improved  
849 methods for observing Earth's time variable mass distribution with GRACE using spherical  
850 cap mascons, *J. Geophys. Res. Solid Earth*, 120, 2648–2671, doi:10.1002/2014JB011547,  
851 2015.
- 852 Xie, H., Longuevergne, L., Ringler, C., and Scanlon, B. R.: Calibration and evaluation of a semi-  
853 distributed watershed model of Sub-Saharan Africa using GRACE data, *Hydrol. Earth Syst.*  
854 *Sci.*, 16, 3083-3099, 2012.
- 855 Yin, X., and Nicholson, S. E.: The water balance of Lake Victoria, *Hydrol. Sci. J.*, 43, 789-811,  
856 1998.
- 857
- 858



859 **Figure Captions**

860

861 **Figure 1.** Map of the study area encompassing the Lake Victoria Basin (LVB) and Lake Kyoga  
862 Basin (LKB), and location of the in situ monitoring stations. The Upper Nile Basin is marked by  
863 a rectangle (red) within the entire Nile River Basin shown as a shaded relief index map.  
864 Piezometric monitoring (red circles) and lake-level gauging (dark blue squares) stations are  
865 shown on the map.

866

867 **Figure 2.** Observed daily total dam releases (blue line) and the agreed curve (red line) at the  
868 outlet of Lake Victoria in Jinja from November 2007 to July 2009 (Owor et al., 2011).

869

870 **Figure 3.** Mean annual rainfall for the period of 2003–2012 derived from TRMM satellite  
871 observations. Greater annual rainfall is observed over much of the Lake Victoria and  
872 northeastern corner of the Lake Victoria Basin.

873

874 **Figure 4.** Seasonal pattern of TRMM-derived monthly rainfall, various GRACE-derived  $\Delta$ TWS  
875 signals [GRCE=ensemble mean of CSR, GFZ, and JPL; GRGS and JPL-Mascons (MSCN)  
876 products], GLDAS LSMs ensemble  $\Delta$ SMS, in situ  $\Delta$ SWS and  $\Delta$ GWS over the Lake Victoria  
877 Basin.

878

879 **Figure 5.** Monthly time-series datasets for the Lake Victoria Basin (LVB) from January 2003 to  
880 December 2012: (a) *GRCTellus* GRACE-derived  $\Delta$ TWS (ensemble mean of CSR, GFZ, and  
881 JPL), GRGS and JPL-Mascons  $\Delta$ TWS time-series data; (b) GLDAS-derived  $\Delta$ SMS (ensemble  
882 mean of NOAH, CLM, and VIC); (c) lake-level-derived  $\Delta$ SWS; and (d) borehole-derived  $\Delta$ GWS  
883 time-series data.

884

885 **Figure 6.** Monthly time-series datasets for the Lake Kyoga Basin (LKB) from January 2003 to  
886 December 2012: (a) *GRCTellus* GRACE-derived  $\Delta$ TWS (ensemble mean of CSR, GFZ, and  
887 JPL), GRGS and JLP-Mascons  $\Delta$ TWS time-series data; (b) GLDAS-derived  $\Delta$ SMS (ensemble  
888 mean of NOAH, CLM, and VIC); (c) lake-level-derived  $\Delta$ SWS; and (d) borehole-derived  $\Delta$ GWS  
889 time-series data.



890 **Figure 7.** Comparison among time-series records of  $\Delta$ TWS from *GRCTellus* (ensemble mean of  
891 CSR, GFZ, and JPL), GRGS and JPL-MASCON GRACE products and in situ  $\Delta$ TWS for the  
892 Lake Victoria Basin (LVB) (a) and Lake Kyoga Basin (LKB), (b) for the period of 2003 to 2012.  
893 The vertical grey lines represent monthly rainfall anomalies in LVB and LKB.

894

895 **Figure 8.** Estimates of in situ  $\Delta$ GWS and GRACE-derived  $\Delta$ GWS time-series records  
896 (2003–2012) in LVB show a substantial variations among themselves. Note that an adjusted  
897  $\Delta$ SWS (scaling factor of 0.11) is applied in the disaggregation of  $\Delta$ GWS using *GRCTellus*  
898 GRACE (ensemble mean of CSR, GFZ, and JPL) product; similarly, an adjusted  $\Delta$ SWS (scaling  
899 factor of 0.39) is applied for the JPL-Mascons product.

900

901 **Figure 9.** Taylor diagram shows strength of statistical association, variability in amplitudes of  
902 time-series records and agreement among the reference data, in situ  $\Delta$ TWS and *GRCTellus*  
903 GRACE-derived  $\Delta$ TWS (ensemble mean of CSR, GFZ, and JPL, GRGS and Mascons  $\Delta$ TWS  
904 time-series records), simulated  $\Delta$ SMS (ensemble mean of NOAH, CLM, and VIC), in situ  
905  $\Delta$ SWS, and in situ  $\Delta$ GWS over the LVB. The solid arcs around the reference point (black  
906 square) indicate centered Root Mean Square (RMS) differences among in situ  $\Delta$ TWS and other  
907 variables, and the dashed arcs from the origin of the diagram indicate variability in time-series  
908 records. Data for Lake Victoria Basin (LVB) are only shown in this diagram.

909



910 **Table 1.** Estimated areal extent (km<sup>2</sup>) of the Lake Victoria Basin (LVB), Lake Kyoga Basin  
 911 (LKB), Lake Victoria and Lake Kyoga.

912

Basin/Lake	This study	UNEP (2013)	Awange et al. (2014)
Lake Victoria Basin	256 100	184 000	258 000
Lake Victoria	67 220	68 800	-
Lake Kyoga Basin	79 270	75 000	75 000
Lake Kyoga	2 730	1 720	-

913

914

915

916 **Table 2.** Details of groundwater and lake level monitoring stations located in Lake Victoria  
 917 Basin and Lake Kyoga Basin.

918

Monitoring Station	Basin	Parameter	Longitude	Latitude	Depth (m bgl)
Apac	LKB	Groundwater level	32.50	1.99	15.0
Pallisa	LKB	Groundwater level	33.69	1.20	46.2
Soroti	LKB	Groundwater level	33.63	1.69	66.0
Bugondo	LKB	Lake level	33.20	0.45	-
Entebbe	LVB	Groundwater level	32.47	0.04	48.0
Rakai	LVB	Groundwater level	31.40	-0.69	53.0
Nkokonjeru	LVB	Groundwater level	32.91	0.24	30.0
Jinja	LVB	Lake level	33.23	1.59	-

919



920 **Table 3.** Linear trends ( $\text{cm yr}^{-1}$ ) in GRACE  $\Delta\text{TWS}$  and in situ  $\Delta\text{TWS}$  in Lake Victoria Basin and  
 921 Lake Kyoga Basin over various time periods (statistically significant trends,  $p$  values  $<0.05$  are  
 922 marked by an asterisk).

Period	GRACE Ensemble	GRGS	JPL-Mascons	In situ TWS
Lake Victoria Basin (LVB)				
2003–2006	−4.10*	−9.00*	−7.70*	−11.00*
2007–2012	−0.31	1.50*	1.90*	1.10*
2003–2012	0.04	0.58	0.79*	0.54*
Lake Kyoga Basin (LKB)				
2003–2006	−2.10*	−4.60*	−5.60*	−2.80*
2007–2012	0.22	2.00*	2.20*	0.48
2003–2012	−0.01	0.54*	0.55*	−0.56*

923

924





925

926

927

928

929

930

931

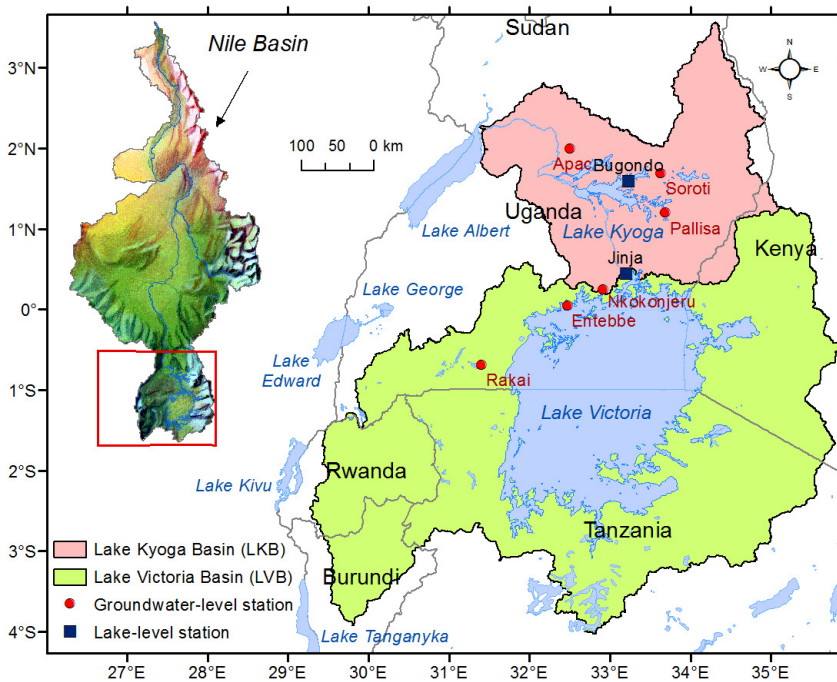
932

933

934

935

936



937

938

939

940

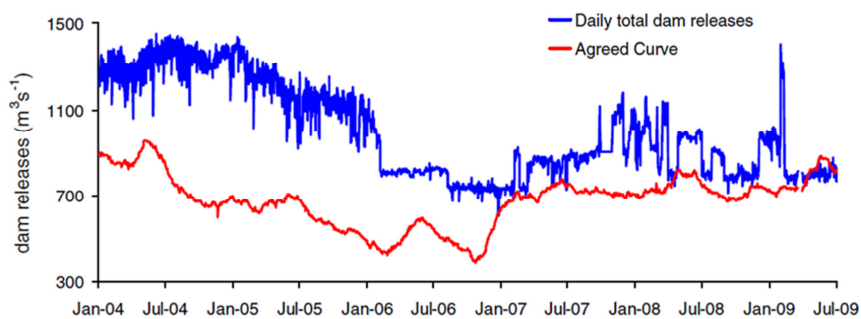
941

942

**Figure 1.** Map of the study area encompassing the Lake Victoria Basin (LVB) and Lake Kyoga Basin (LKB), and location of the in situ monitoring stations. The Upper Nile Basin is marked by a rectangle (red) within the entire Nile River Basin shown as a shaded relief index map. Piezometric monitoring (red circles) and lake-level gauging (dark blue squares) stations are shown on the map.



943  
944  
945  
946  
947  
948  
949  
950  
951  
952  
953  
954



955 **Figure 2.** Observed daily total dam releases (blue line) and the agreed curve (red line) at the  
956 outlet of Lake Victoria in Jinja from November 2007 to July 2009 (Owor et al., 2011).



957  
958  
959  
960  
961  
962  
963  
964  
965  
966  
967  
968  
969  
970  
971  
972  
973  
974  
975  
976  
977

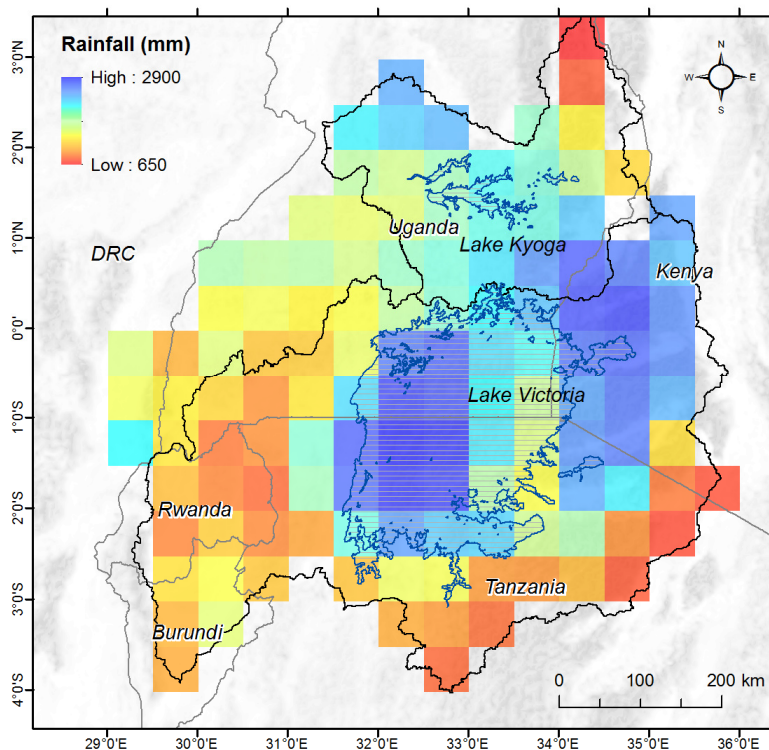


**Figure 3.** Mean annual rainfall for the period of 2003–2012 derived from TRMM satellite observations. Greater annual rainfall is observed over much of the Lake Victoria and northeastern corner of the Lake Victoria Basin.



978  
 979  
 980  
 981  
 982  
 983  
 984  
 985  
 986  
 987  
 988  
 989  
 990  
 991  
 992  
 993  
 994  
 995

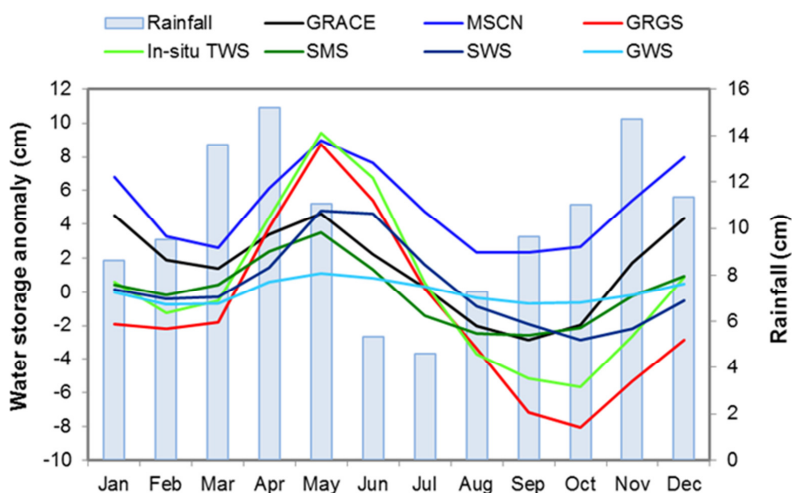


**Figure 4.** Seasonal pattern of TRMM-derived monthly rainfall, various GRACE-derived  $\Delta$ TWS signals [GRCE=ensemble mean of CSR, GFZ, and JPL; GRGS and JPL-Mascons (MSCN) products], GLDAS LSMs ensemble  $\Delta$ SMS, in situ  $\Delta$ SWS and  $\Delta$ GWS over the Lake Victoria Basin.



996  
 997  
 998  
 999  
 1000  
 1001  
 1002  
 1003  
 1004  
 1005  
 1006  
 1007  
 1008  
 1009  
 1010  
 1011  
 1012  
 1013  
 1014  
 1015  
 1016  
 1017  
 1018  
 1019  
 1020  
 1021  
 1022  
 1023  
 1024  
 1025  
 1026

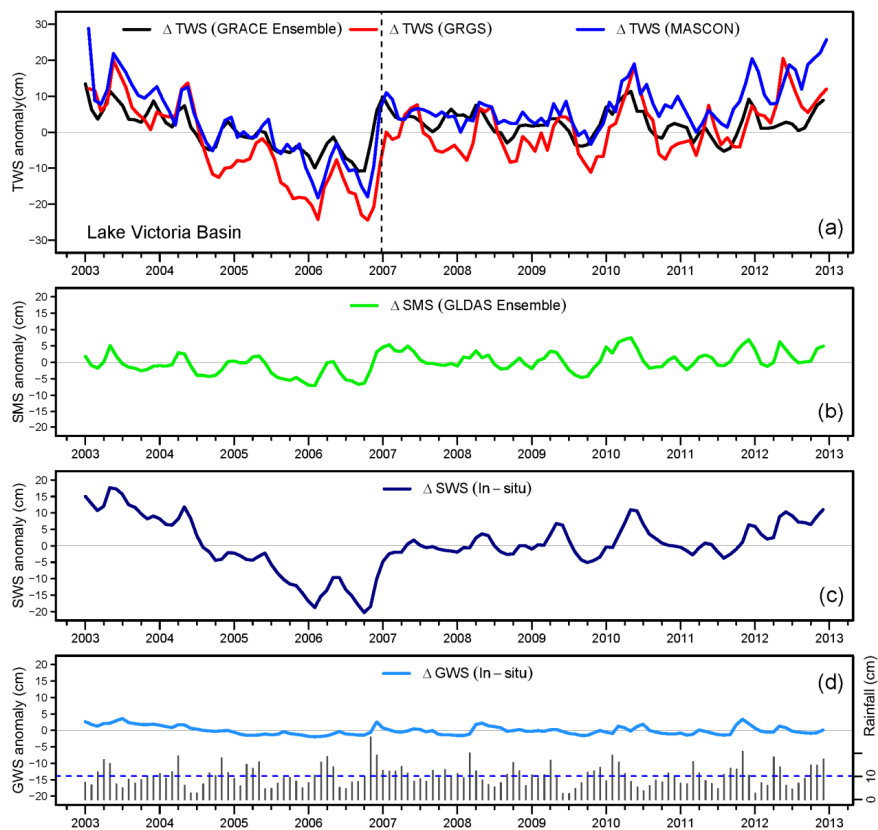


**Figure 5.** Monthly time-series datasets for the Lake Victoria Basin (LVB) from January 2003 to December 2012: (a) *GRCTellus* GRACE-derived  $\Delta$ TWS (ensemble mean of CSR, GFZ, and JPL), GRGS and JPL-Mascons  $\Delta$ TWS time-series data; (b) GLDAS-derived  $\Delta$ SMS (ensemble mean of NOAA, CLM, and VIC); (c) lake-level-derived  $\Delta$ SWS; and (d) borehole-derived  $\Delta$ GWS time-series data.



1027

1028

1029

1030

1031

1032

1033

1034

1035

1036

1037

1038

1039

1040

1041

1042

1043

1044

1045

1046

1047

1048

1049

1050

1051

1052

1053

1054

1055

1056

1057

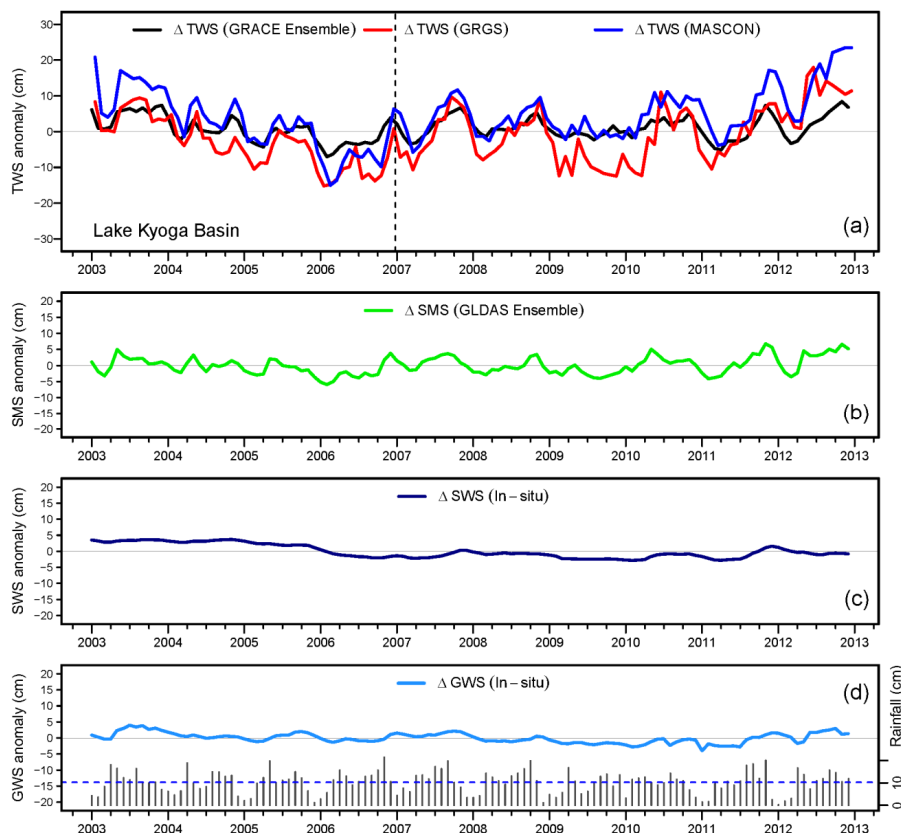


**Figure 6.** Monthly time-series datasets for the Lake Kyoga Basin (LKB) from January 2003 to December 2012: (a) *GRCTellus* GRACE-derived  $\Delta$ TWS (ensemble mean of CSR, GFZ, and JPL), GRGS and JLP-Mascons  $\Delta$ TWS time-series data; (b) GLDAS-derived  $\Delta$ SMS (ensemble mean of NOAA, CLM, and VIC); (c) lake-level-derived  $\Delta$ SWS; and (d) borehole-derived  $\Delta$ GWS time-series data.



1058

1059

1060

1061

1062

1063

1064

1065

1066

1067

1068

1069

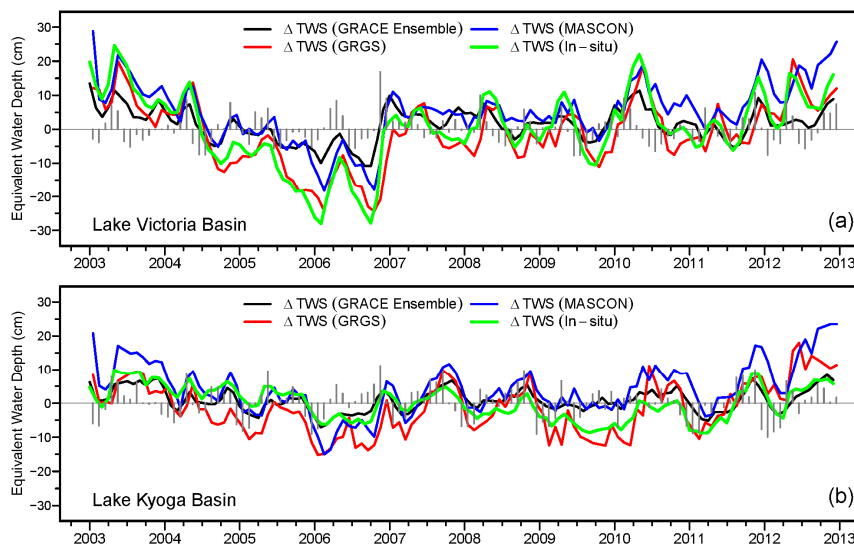
1070

1071

1072

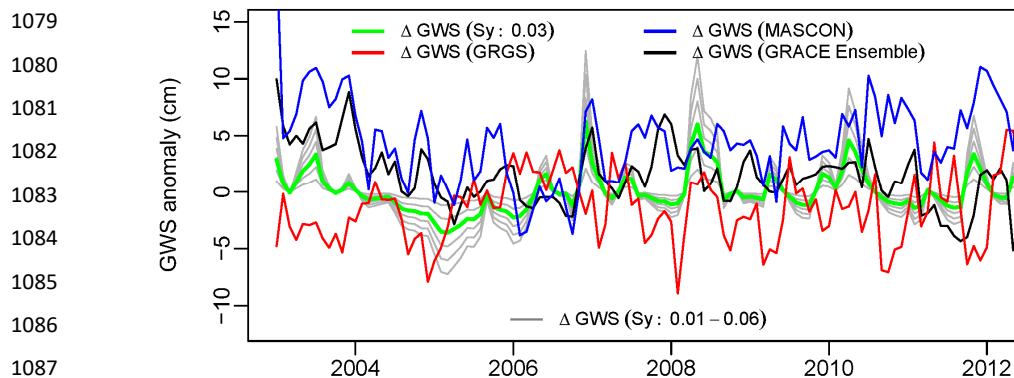
1073 **Figure 7.** Comparison among time-series records of  $\Delta$ TWS from *GRCTellus* (ensemble mean of  
1074 CSR, GFZ, and JPL), GRGS and JPL-MASCON GRACE products and in situ  $\Delta$ TWS for the  
1075 Lake Victoria Basin (LVB) (a) and Lake Kyoga Basin (LKB), (b) for the period of 2003 to 2012.  
1076 The vertical grey lines represent monthly rainfall anomalies in LVB and LKB.

1077





1078



1088

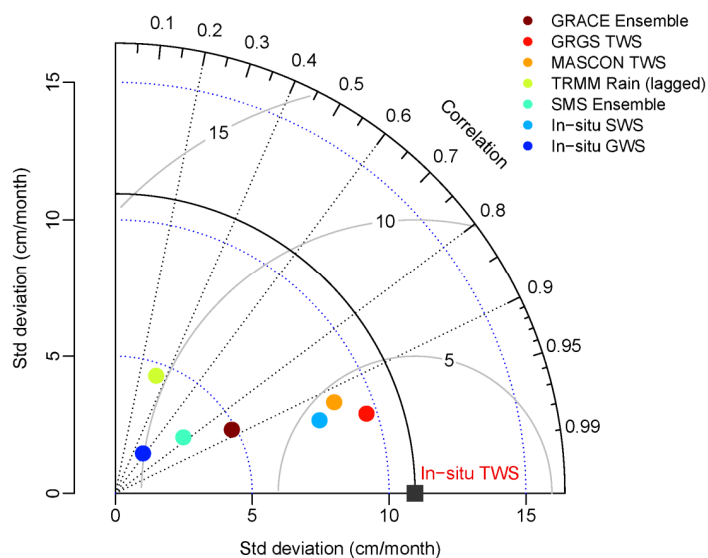
1089 **Figure 8.** Estimates of in situ  $\Delta$ GWS and GRACE-derived  $\Delta$ GWS time-series records  
1090 (2003–2012) in LVB show a substantial variations among themselves. Note that an adjusted  
1091  $\Delta$ SWS (scaling factor of 0.11) is applied in the disaggregation of  $\Delta$ GWS using *GRCTellus*  
1092 GRACE (ensemble mean of CSR, GFZ, and JPL) product; similarly, an adjusted  $\Delta$ SWS (scaling  
1093 factor of 0.39) is applied for the JPL-Mascons product.

1094





1095  
 1096  
 1097  
 1098  
 1099  
 1100  
 1101  
 1102  
 1103  
 1104  
 1105  
 1106  
 1107  
 1108  
 1109  
 1110  
 1111



1112 **Figure 9.** Taylor diagram shows strength of statistical association, variability in amplitudes of  
 1113 time-series records and agreement among the reference data, in situ  $\Delta$ TWS and *GRCTellus*  
 1114 GRACE-derived  $\Delta$ TWS (ensemble mean of CSR, GFZ, and JPL, GRGS and Mascons  $\Delta$ TWS  
 1115 time-series records), simulated  $\Delta$ SMS (ensemble mean of NOAH, CLM, and VIC), in situ  
 1116  $\Delta$ SWS, and in situ  $\Delta$ GWS over the LVB. The solid arcs around the reference point (black  
 1117 square) indicate centered Root Mean Square (RMS) differences among in situ  $\Delta$ TWS and other  
 1118 variables, and the dashed arcs from the origin of the diagram indicate variability in time-series  
 1119 records. Data for Lake Victoria Basin (LVB) are only shown in this diagram.